A Wavelet-based Multifractal Analysis for scalar and vector fields: Application to developped turbulence

Pierre Kestener*, Alain Arneodo

Laboratoire de Physique, ENS Lyon, France

* *present address: CEA Saclay, DSM/DAPNIA/SEDI, Gif-Sur-Yvette, FRANCE*

Contents

- Introduction
- Characterization of multifractal images with the 2D WTMM method
- Generalizations of the WTMM method $\longrightarrow$ from 2D to 3D

  $\longrightarrow$ from scalar to vector

  - Application to developped turbulence (direct numerical simulations)

    3D scalar case : dissipation field and enstrophy field

    3D vector case : velocity field and vorticity field
  - Application to galaxy distribution (simulation data)

Fractal Objects : self-similarity

- exact self-similarity :

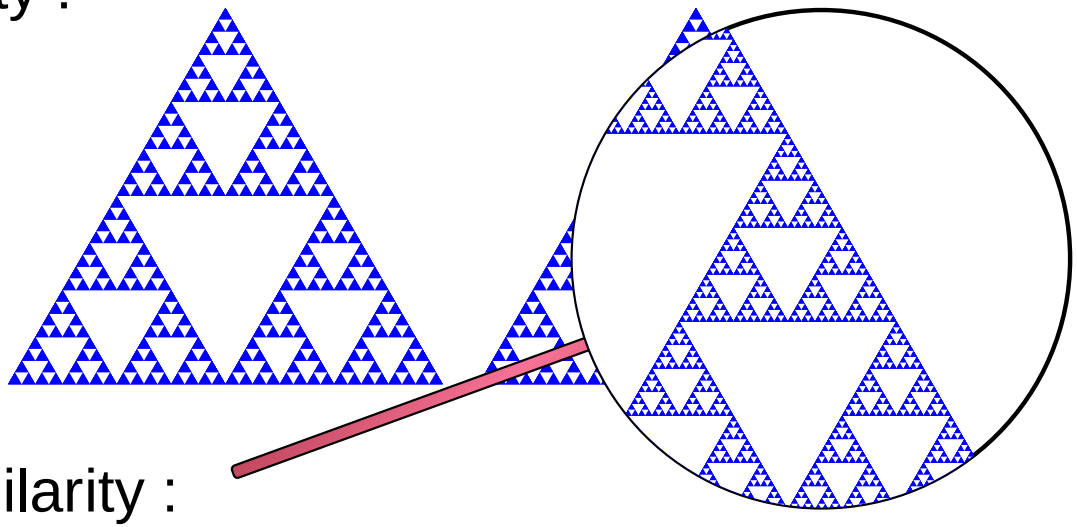

- statistical self-similarity :

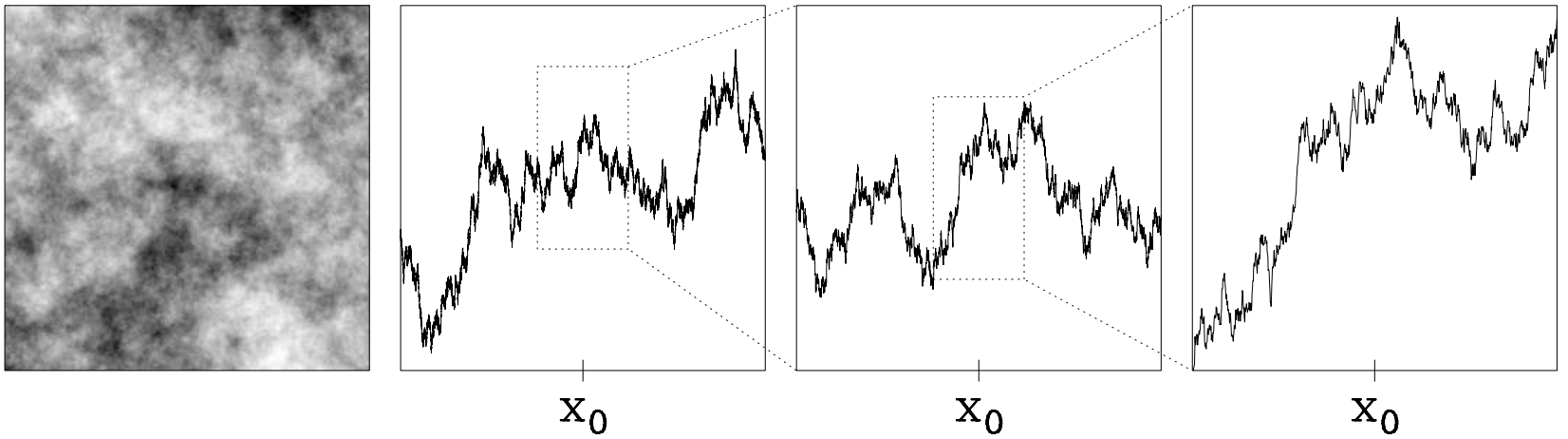

$$f(x_0 + \lambda u) - f(x_0) \sim \lambda^{h(x_0)} (f(x_0 + u) - f(x_0))$$

Self-similarity and Wavelet Transform

- **Wavelet Transform :** a mathematical microscope to study fractal objects self-similarity properties

$$\mathrm{T}_\psi[f](a,b) =< f, \psi_{a,b} >= \frac{1}{\sqrt{a}} \int_{-\infty}^{+\infty} dx\, f(x) \psi^*(\frac{x-b}{a})$$

- local self-similarity (Hölder exponent) can be seen in the wavelet transform coefficients under scaling laws (Jaffard, Mallat et coll., Holschneider and Tchamitchian) :

$$\mathrm{T}_\psi[f](a,x_0) \sim a^{h(x_0)+\frac{1}{2}}, \quad a \longrightarrow 0^+$$

- **statistical description of self-similarity :**

  WTMM method (Wavelet Transform Modulus Maxima) by Muzy, Bacry, Arnéodo (1993) for multifractal signals.

- many applications in bioinformatics (DNA Sequences), in turbulence, in finance, in geophysics,...

classical multifractal formalism comes from turbulence

- **The Navier-Stokes equations:**

$$\partial_t \mathbf{u} + \mathbf{u}.\nabla\ \mathbf{u} = -\frac{1}{\rho}\nabla p + \mathbf{f} + \nu\mathbf{\Delta u}, \qquad +\nabla.\mathbf{u} = 0 + BC + CI$$

- **turbulent regime :** $||\mathbf{u}.\nabla\ \mathbf{u}|| >> ||\nu\mathbf{\Delta u}||$
- **signal highly disorganized and structures at all scales, unpredictable as for details**

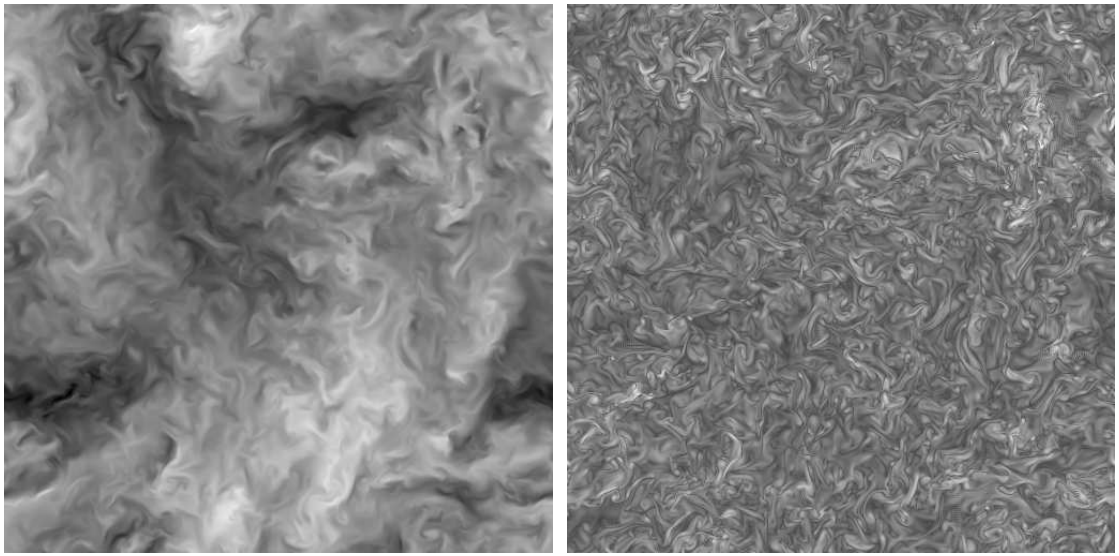

☞ **Statistical tools required**

Multifractal description of intermittency in turbulence

Multifractal description of intermittency in turbulence

- **classical multifractal formalism comes from turbulence**
  - ☞ **multifractal model for velocity : longitudinal structure functions based on (1D) velocity increments :**

$$S_p(l) \;=\; < (\mathrm{e}.\delta \mathrm{v}(\mathrm{r}, l\mathrm{e}))^p > \;\sim\; l^{\zeta_p}, \qquad p > 0$$

  - ☞ **multifractal model for (1D *surrogate*) dissipation : RSH hypothesis**

$$S_p(l) \;\sim\; < \varepsilon_l^{p/3} > l^{p/3} \;\sim\; l^{\tau_\varepsilon(p/3)+p/3}.$$

  Measure of the spectra $\tau_\varepsilon(p)$ and $f(\alpha)$ with the box-counting method.

- **multifractal formalism based on WT (WTMM method) for regularity analysis of functions, measures and distributions.**

  - ☞ **generalization of the WTMM method 1D/2D⟶3D**
  - ☞ **generalization to multidimensional vector fields. First application to velocity and vorticity fields from numerical turbulent flows.**

2D WTMM Methodology : PhD work of N. Decoster

2D data : I

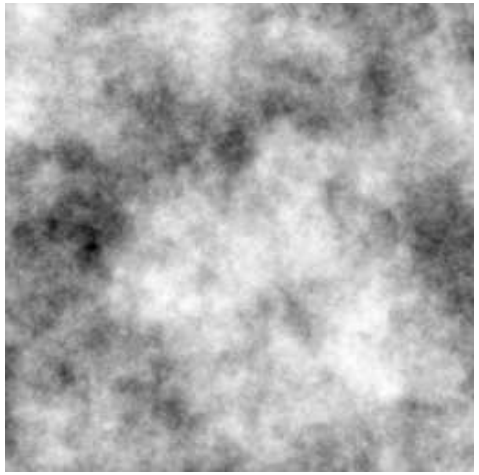

Smoothing scale a →

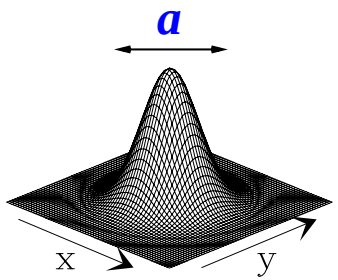

Gradient ∇ →

$$\left[\frac{\partial}{\partial x}, \frac{\partial}{\partial y}\right]$$

Wavelet Transform

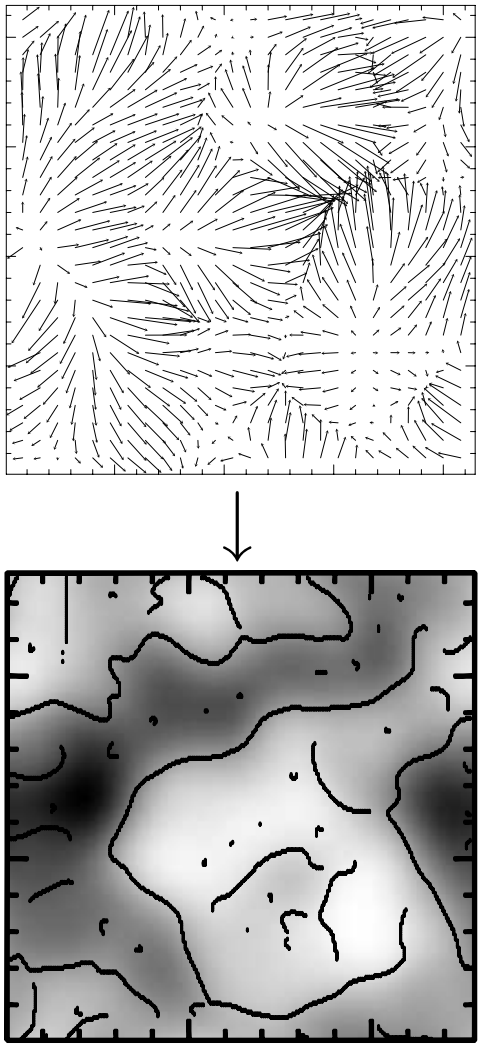

$$\mathbf{T}_\psi(\mathrm{r}, a) = \begin{pmatrix} I * \frac{\partial \phi_a}{\partial x}(\mathrm{r}) \\ I * \frac{\partial \phi_a}{\partial y}(\mathrm{r}) \end{pmatrix}$$

$$\mathbf{T}_\psi(\mathrm{r}, a) = \nabla (I * \phi_a)(\mathrm{r}) = (\mathcal{M}_\psi(\mathrm{r}, a), \mathcal{A}_\psi(\mathrm{r}, a))$$

WTMM Methodology : Skeleton

WTMM Chains

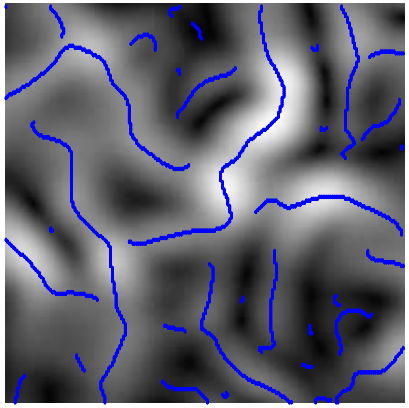

WTMMM

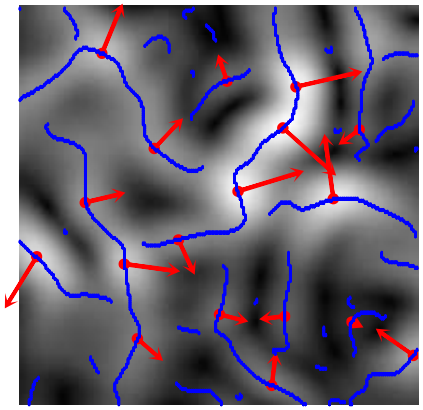

WTMM Chains at 3 different scales

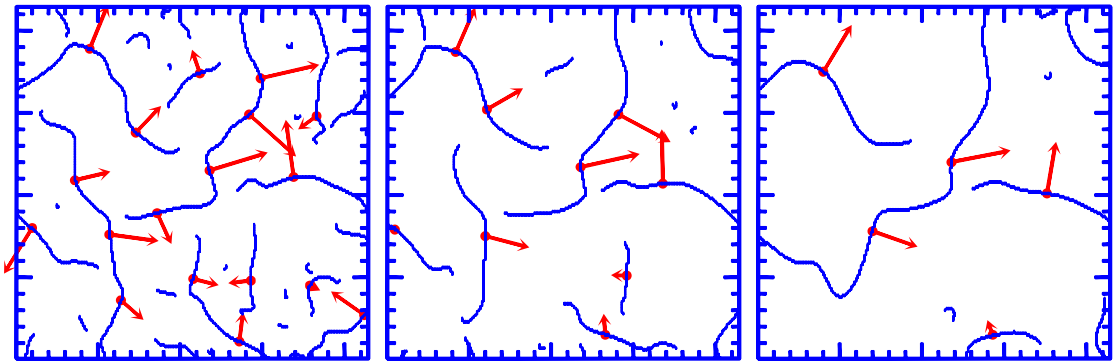

WTMMM linking : WT skeleton

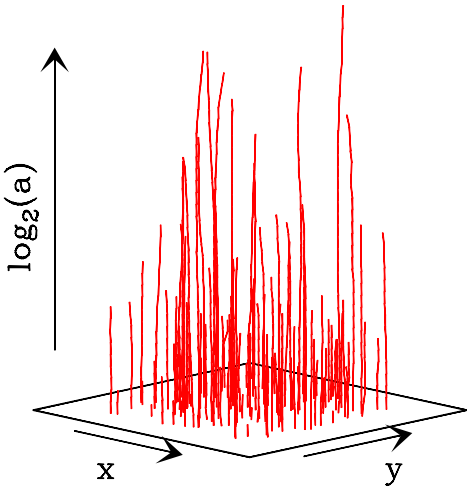

Local roughness characterization : Hölder exponent

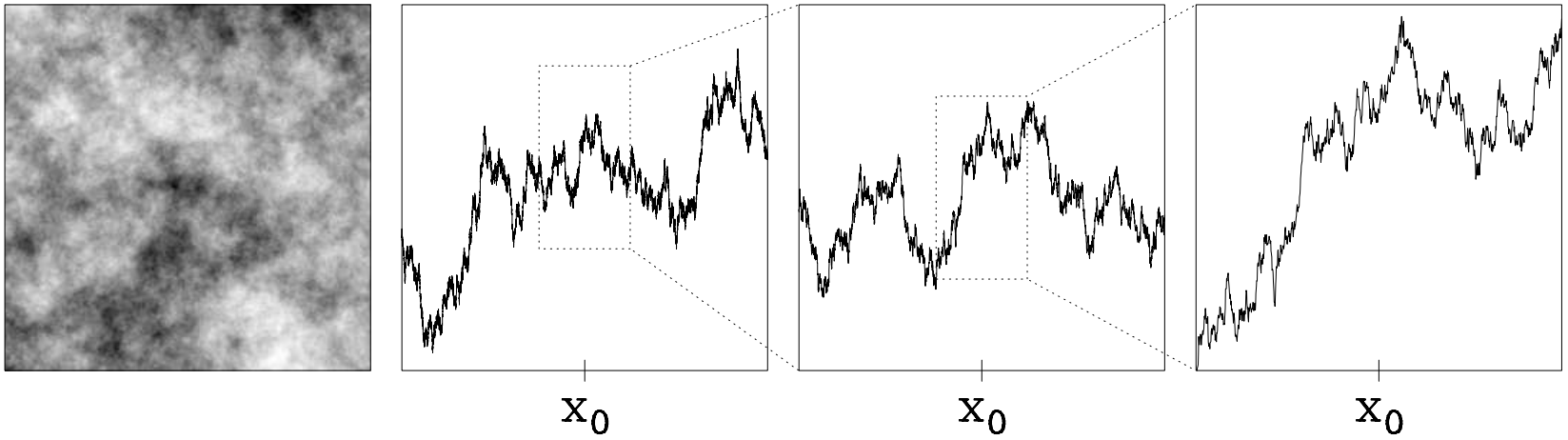

$$f(\mathbf{x_0} + \boldsymbol{\lambda}\mathbf{u}) - f(\mathbf{x_0}) \sim \boldsymbol{\lambda}^{\boldsymbol{h(x_0)}}(f(\mathbf{x_0} + \mathbf{u}) - f(\mathbf{x_0}))$$

- **Monofractal Image**

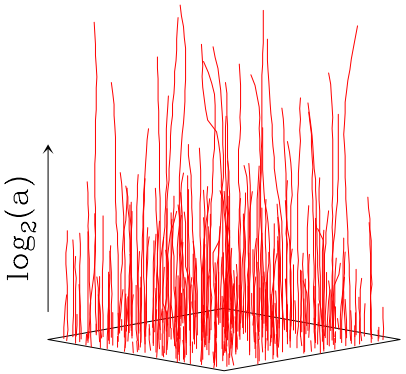

$\mathcal{M} \sim a^{\boldsymbol{h}}$,
single $\boldsymbol{h}$

- **Multifractal Image**

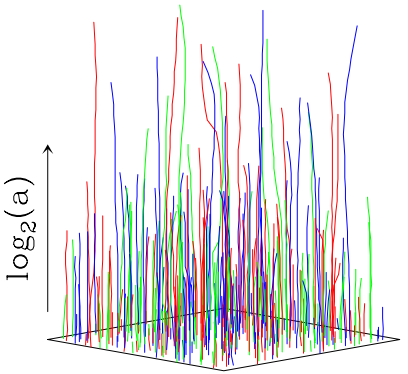

$\mathcal{M} \sim a^{\boldsymbol{h}}, a^{\boldsymbol{h}}, a^{\boldsymbol{h}}$,
$h \in [h_{\mathbf{min}}, h_{\mathbf{max}}]$

WTMM Method : multifractal formalism

Singularity spectrum :

$$D(h) = d_H\{\mathrm{r} \in R^d, h(\mathrm{r}) = h\}$$

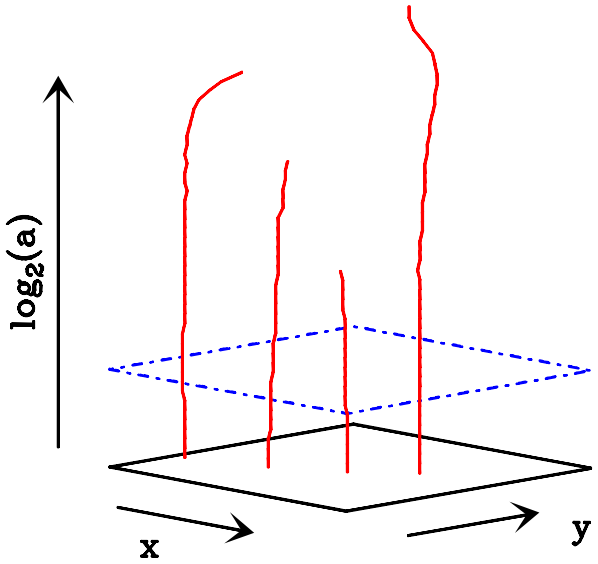

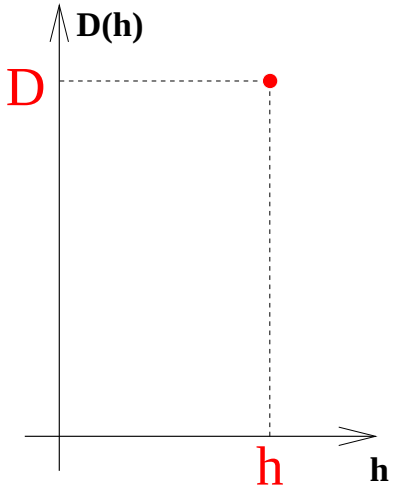

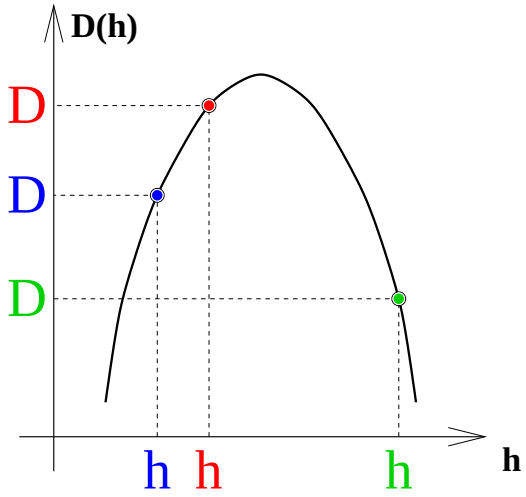

Analogy statistical physics : compute

partition functions

$$\mathcal{Z}(q,a) = \sum_{\mathcal{L}(a)} \left(\mathcal{M}_\psi(\mathrm{r},a)\right)^q \sim a^{\tau(q)}$$

Legendre transform :

$$D(h) = \min_q\left(qh - \tau(q)\right)$$

WTMM Method : multifractal formalism

Singularity spectrum :

$$D(h) = d_H\{\mathrm{r} \in R^d, h(\mathrm{r}) = h\}$$

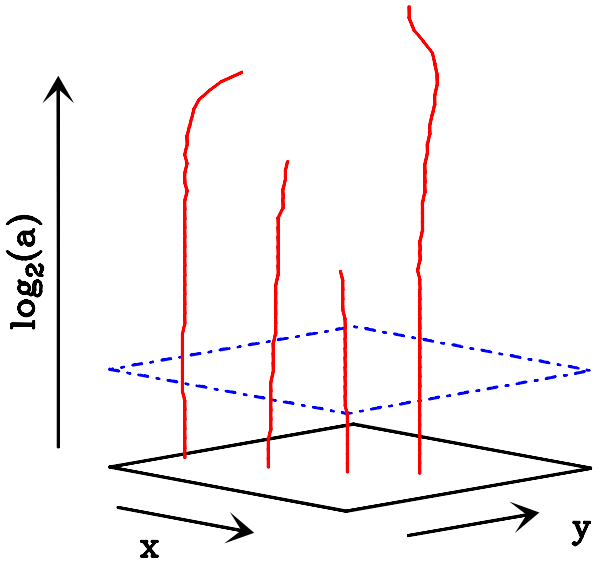

Legendre transform :

$$D(h) = \min_q \left(qh - \tau(q) \right)$$

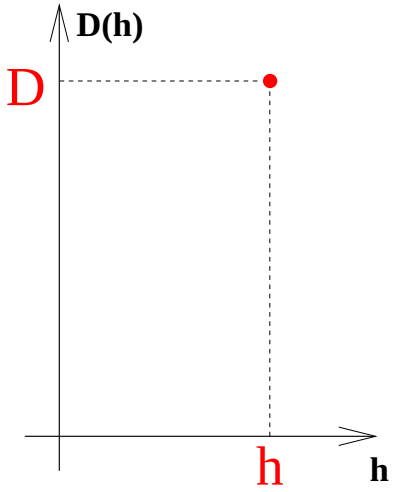

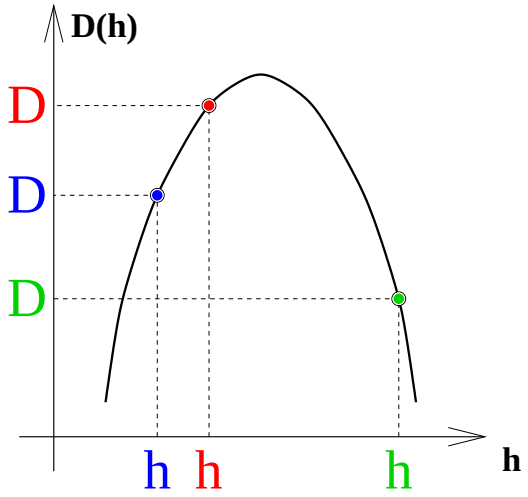

Analogy statistical physics : compute partition functions

$$\mathcal{Z}(q,a) = \sum_{\mathcal{L}(a)} \left(\mathcal{M}_\psi(\mathrm{r},a) \right)^q \sim a^{\tau(q)}$$

$$\mathcal{H}(q,a) = \sum_{\mathcal{L}(a)} \ln |\mathcal{M}_\psi(\mathrm{r},a)| \, \mathcal{W}_\psi(\mathrm{r},a) \sim a^{h(q)}$$

$$\mathcal{D}(q,a) = \sum_{\mathcal{L}(a)} \ln |\mathcal{W}_\psi(\mathrm{r},a)| \, \mathcal{W}_\psi(\mathrm{r},a) \sim a^{D(q)}$$

Application to synthetic monofractal surfaces

fractional Brownian surfaces : $B_H(\mathrm{r})$

- $H < 0.5$: anti-correlated increments
- $H = 0.5$: non-correlated increments
- $H > 0.5$: correlated increments

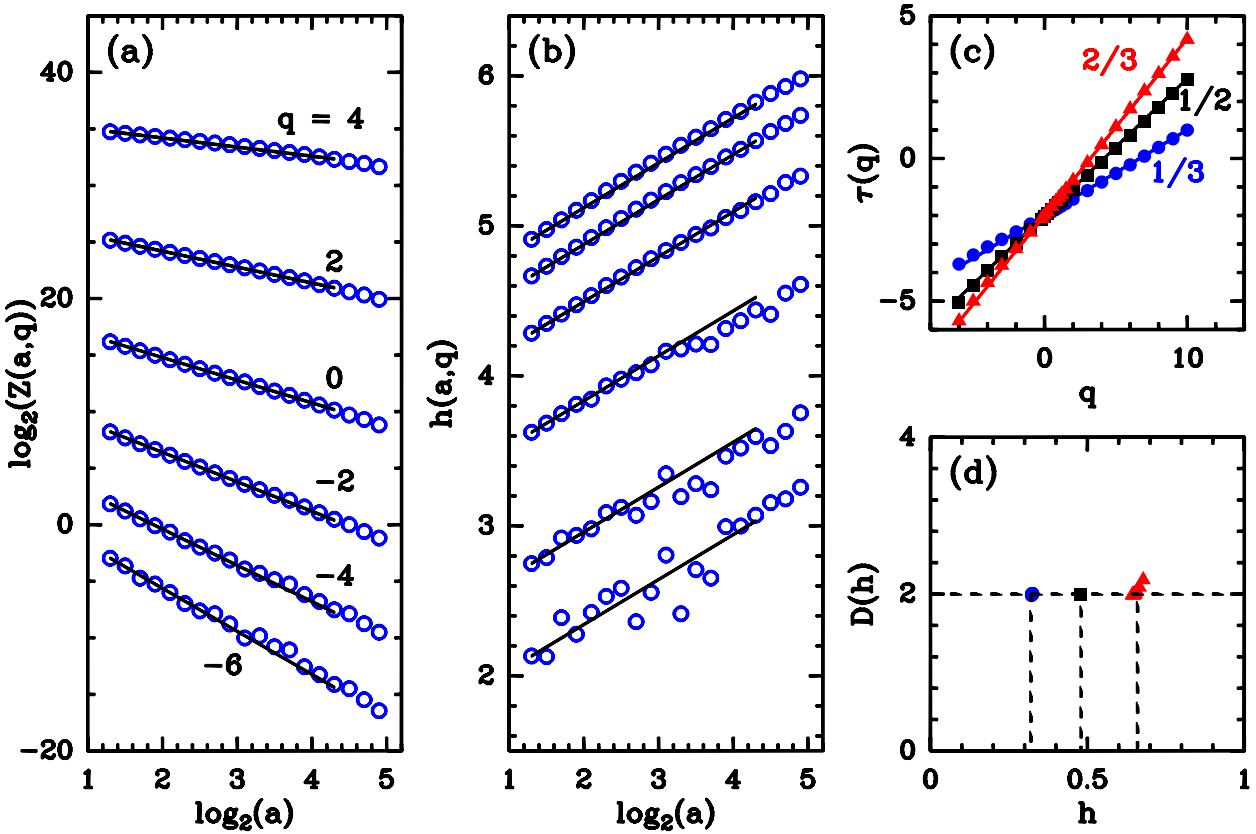

H=1/3

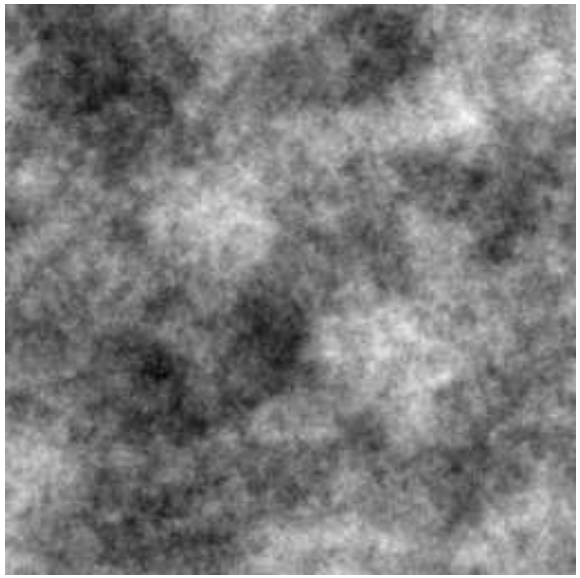

Theoretical Predictions :

- $\tau(q)$ is linear :
  $\tau(q) = qH - 2$
- multifractal spectrum is degenerated :
  $D(h = H) = 2$

Application to synthetic multifractal surfaces

FISC **(Fractionally Integrated Singular Cascades)** model

- simple multiplicative model : p-model or multinomial model

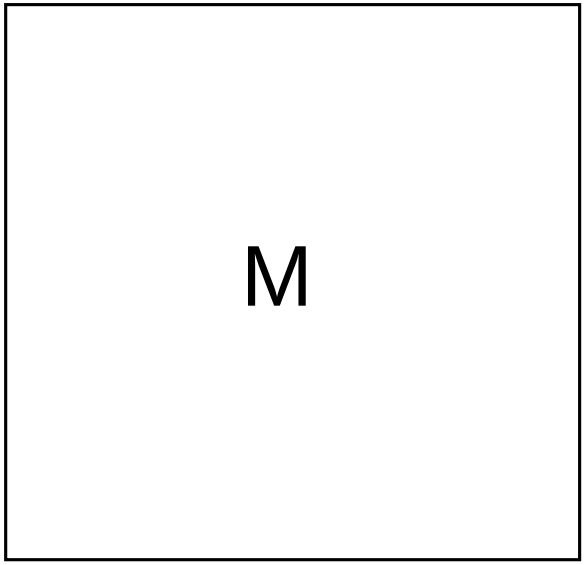

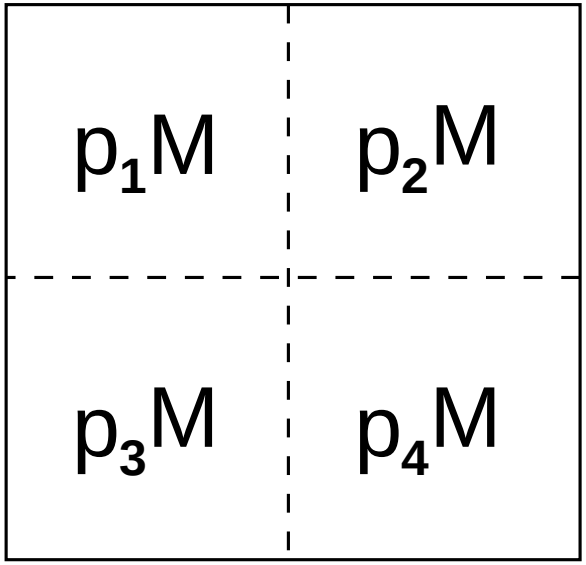

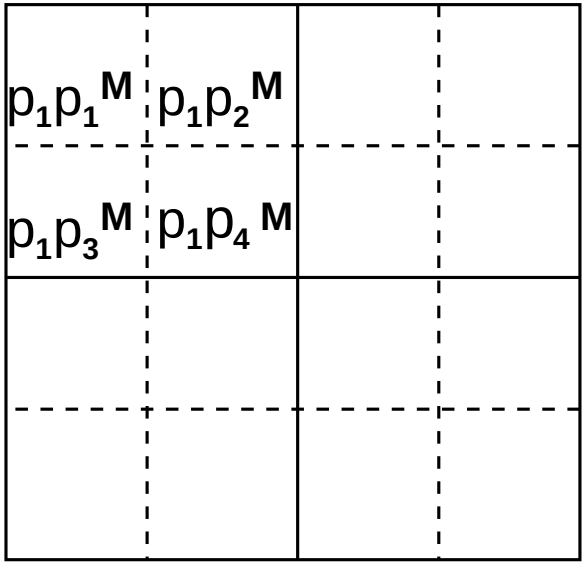

- fractional integration (Fourier domain)
- generalization : p is a random variable with $< p >= 1/4$ (conservative cascading process)

Application to synthetic multifractal surfaces

Multifractal (Fractionally Integrated Singular Cascades) surfaces

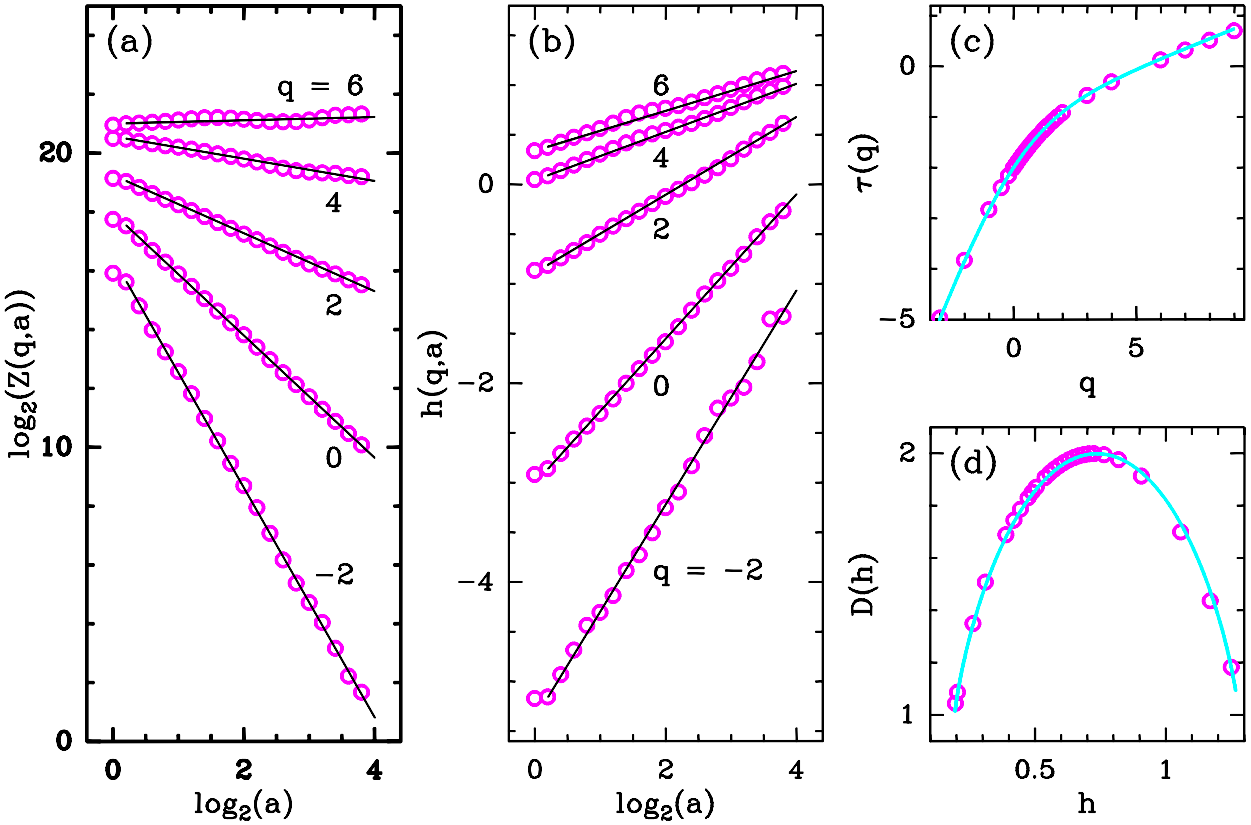

FISC

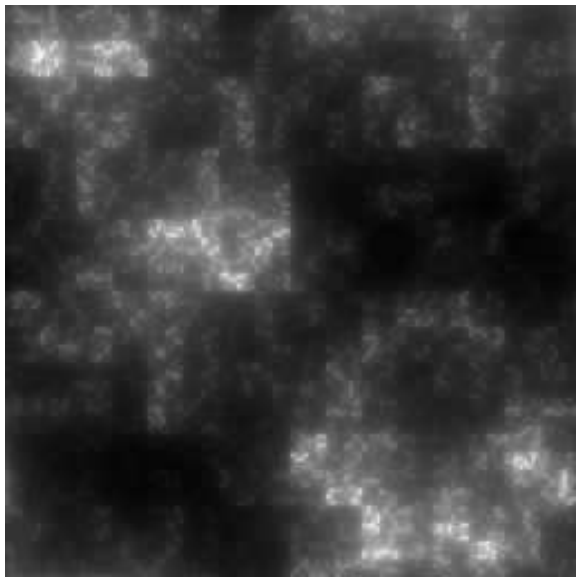

Theoretical predictions :

- $\tau(q)$ is non-linear

$$\tau(q) = -2 - q(1 - H^*) - \log_2(p_1{}^q + p_2{}^q)$$

- singularity spectrum is a non-degenerated convex curve

classical multifractal formalism comes from turbulence

- **The Navier-Stokes equations:**

$$\partial_t \mathbf{u} + \mathbf{u}.\nabla\ \mathbf{u} = -\frac{1}{\rho}\nabla p + \mathbf{f} + \nu\mathbf{\Delta u}, \qquad +\nabla.\mathbf{u} = 0 + BC + CI$$

- **turbulent regime :** $||\mathbf{u}.\nabla\ \mathbf{u}|| >> ||\nu\mathbf{\Delta u}||$
- **signal highly disorganized and structures at all scales, unpredictable as for details**

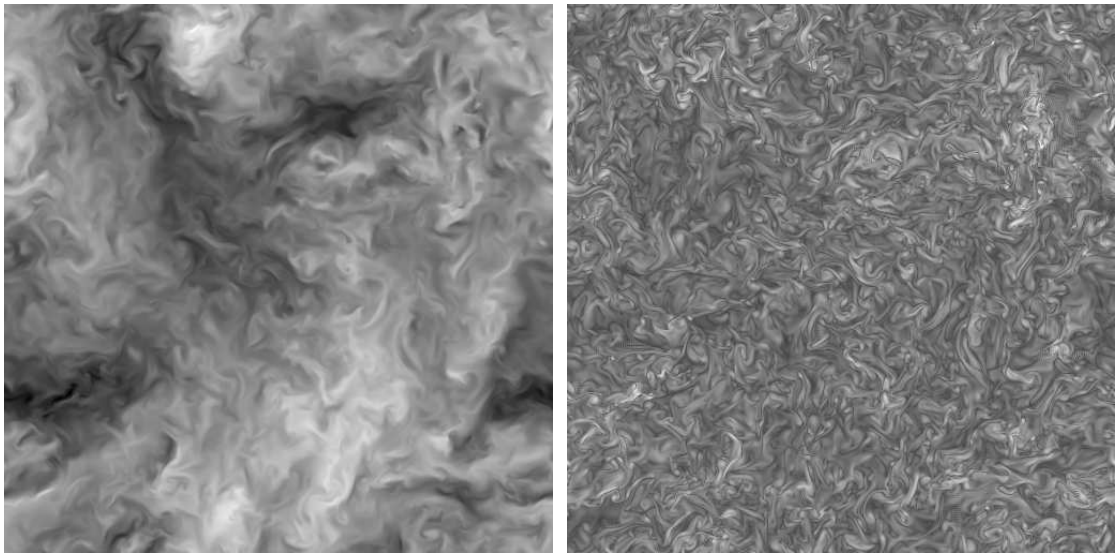

☞ **Statistical tools required**

Multifractal description of intermittency in turbulence

- **classical multifractal formalism comes from turbulence**
  - ☞ **multifractal model for velocity : longitudinal structure functions based on (1D) velocity increments :**

$$S_p(l) \;=\; < (\mathrm{e}.\delta \mathrm{v}(\mathrm{r}, l\mathrm{e}))^p > \;\sim\; l^{\zeta_p}, \qquad p > 0$$

  - ☞ **multifractal model for (1D *surrogate*) dissipation : RSH hypothesis**

$$S_p(l) \;\sim\; < \varepsilon_l^{p/3} > l^{p/3} \;\sim\; l^{\tau_\varepsilon(p/3)+p/3}.$$

  Measure of the spectra $\tau_\varepsilon(p)$ and $f(\alpha)$ with the box-counting method.

- **multifractal formalism based on WT (WTMM method) for regularity analysis of functions, measures and distributions.**

  - ☞ **generalization of the WTMM method 1D/2D⟶3D**
  - ☞ **generalization to multidimensional vector fields. First application to velocity and vorticity fields from numerical turbulent flows.**

3D scalar WTMM method

3D data

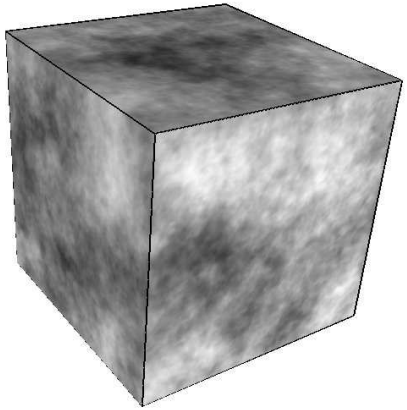

Smoothing scale a $\longrightarrow$ ϕ_a

Gradient ∇ $\longrightarrow$ $\left[\frac{\partial}{\partial x}, \frac{\partial}{\partial y}, \frac{\partial}{\partial z}\right]$

Wavelet Transform

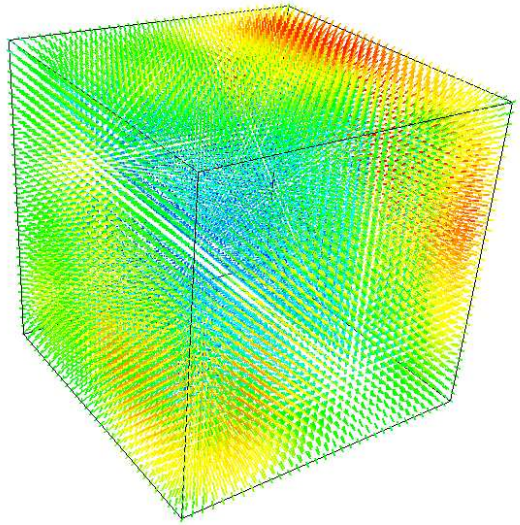

$$\mathbf{T}_{\psi}(\mathbf{r}, a) = \begin{pmatrix} I * \frac{\partial \phi_a}{\partial x}(\mathbf{r}) \\ I * \frac{\partial \phi_a}{\partial y}(\mathbf{r}) \\ I * \frac{\partial \phi_a}{\partial z}(\mathbf{r}) \end{pmatrix} = \nabla\left(I * \phi_a\right)(\mathbf{r})$$

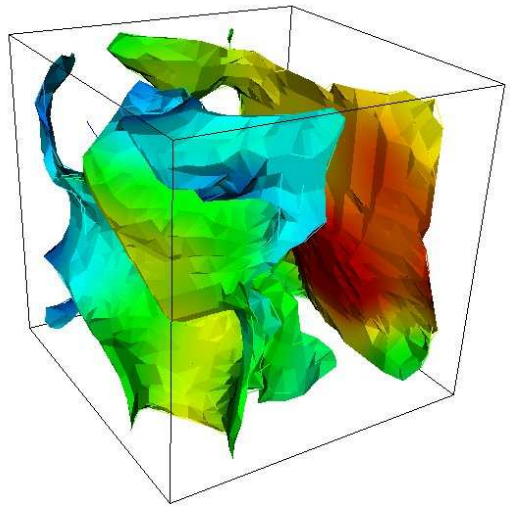

3D scalar WTMM method : skeleton

WTMM surfaces

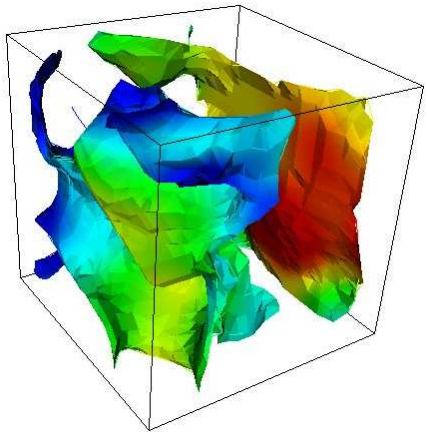

WTMMM points

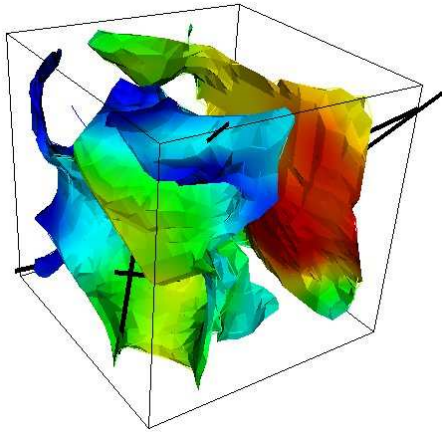

WTMM surfaces at 3 different scales

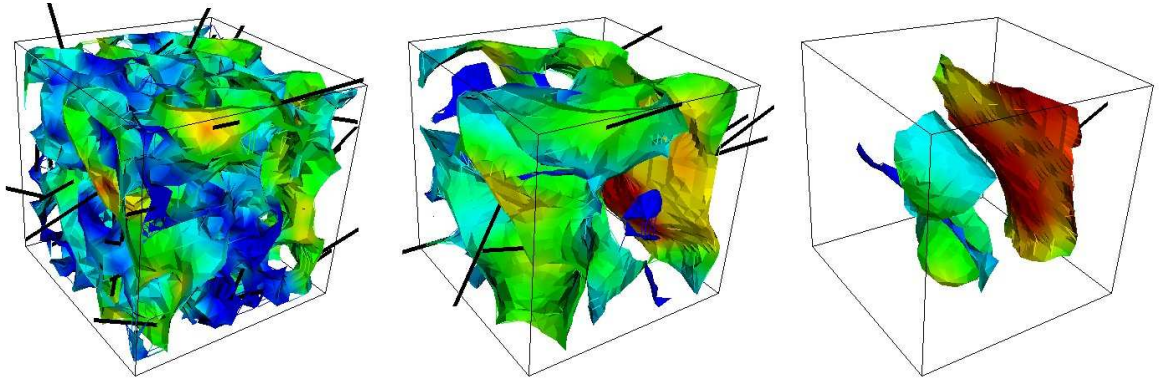

Linking WTMMM : WT Skeleton (projection along z)

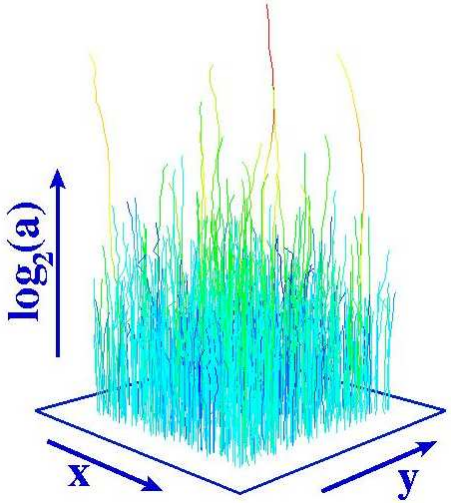

Recursive filters in 3D

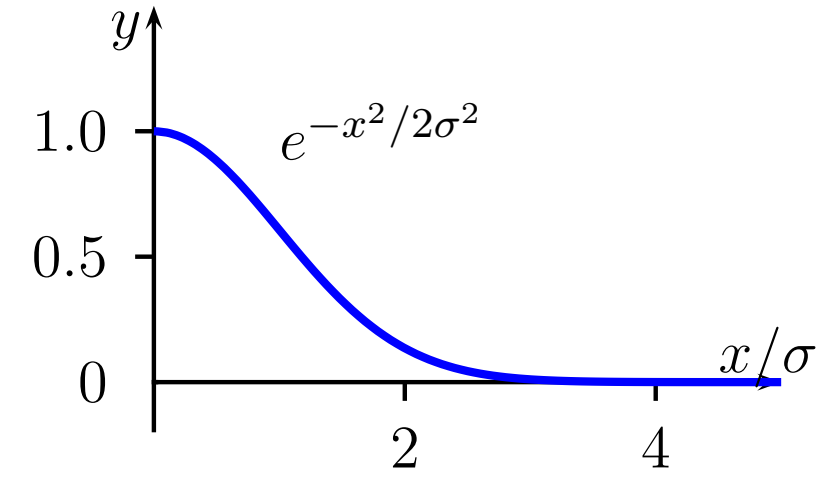

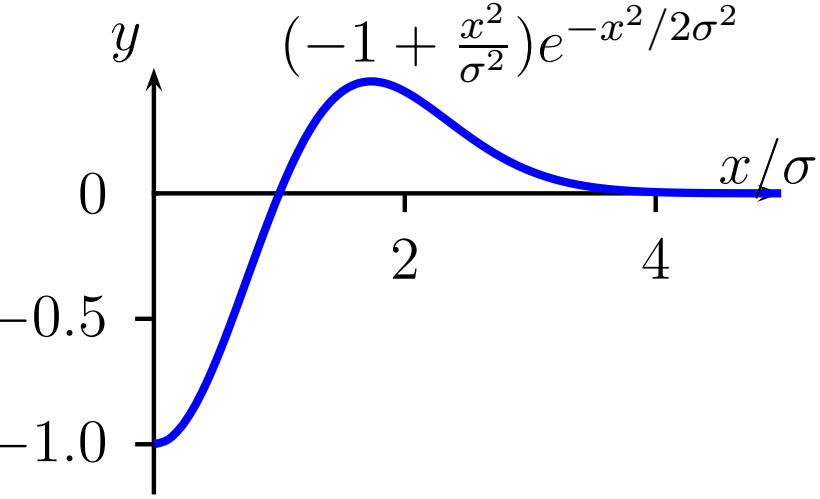

- filters with separated variables
- **Approximate Gaussian filter $e^{-x^2/2\sigma^2}$ with $h_\sigma(x)$**

$$(a_0 \cos(\omega_0 \tfrac{x}{\sigma}) + a_1 \sin(\omega_0 \tfrac{x}{\sigma})) \exp^{-b_0 \frac{x}{\sigma}}$$
$$+(c_0 \cos(\omega_1 \tfrac{x}{\sigma}) + c_1 \sin(\omega_1 \tfrac{x}{\sigma})) \exp^{-b_1 \frac{x}{\sigma}}$$

- **4th order difference equation :**

$$y_k = n_{00}x_k + n_{11}x_{k-1} + n_{22}x_{k-2} + n_{33}x_{k-3} - d_{11}y_{k-1} - d_{22}y_{k-2} - d_{33}y_{k-3} - d_{44}y_{k-4}$$

- **comparison FFT/recursive filters :**

  computing time decrease in 3D case:

  ☞ **60 % for Gaussian filter**

  ☞ **25 % for Mexican filter**

Test-application to synthetic 3D monofractal fields

fractional Brownian fields : $B_H(\mathrm{r})$

- $H < 0.5$: anti-correlated increments
- $H = 0.5$: non-correlated increments
- $H > 0.5$: correlated increments

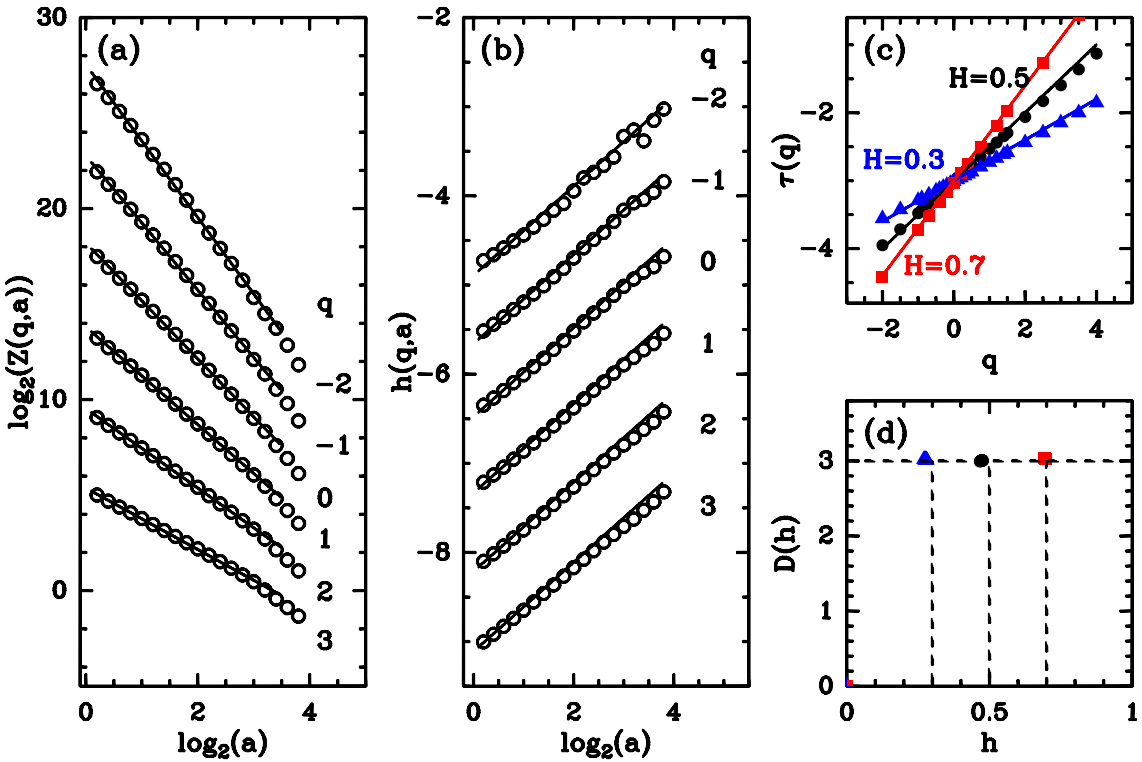

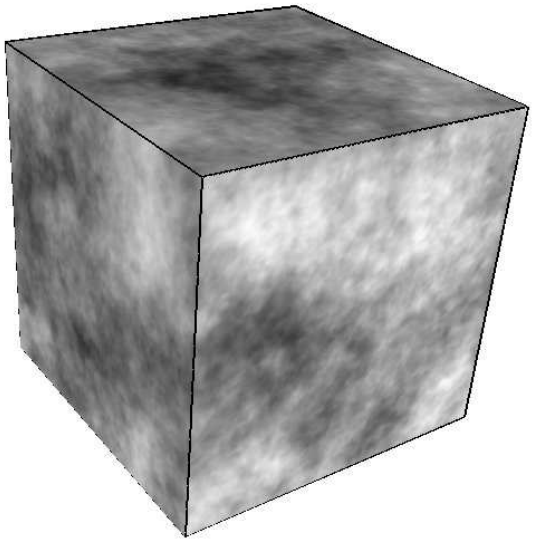

Theoretical predictions :

- $\tau(q)$ is linear: $\tau(q) = qH - 3$
- multifractal spectrum is degenerated: $D(h = H) = 3$

Test-application to synthetic 3D multifractal fields

3D multifractal fields (Fractionally Integrated Singular Cascades)

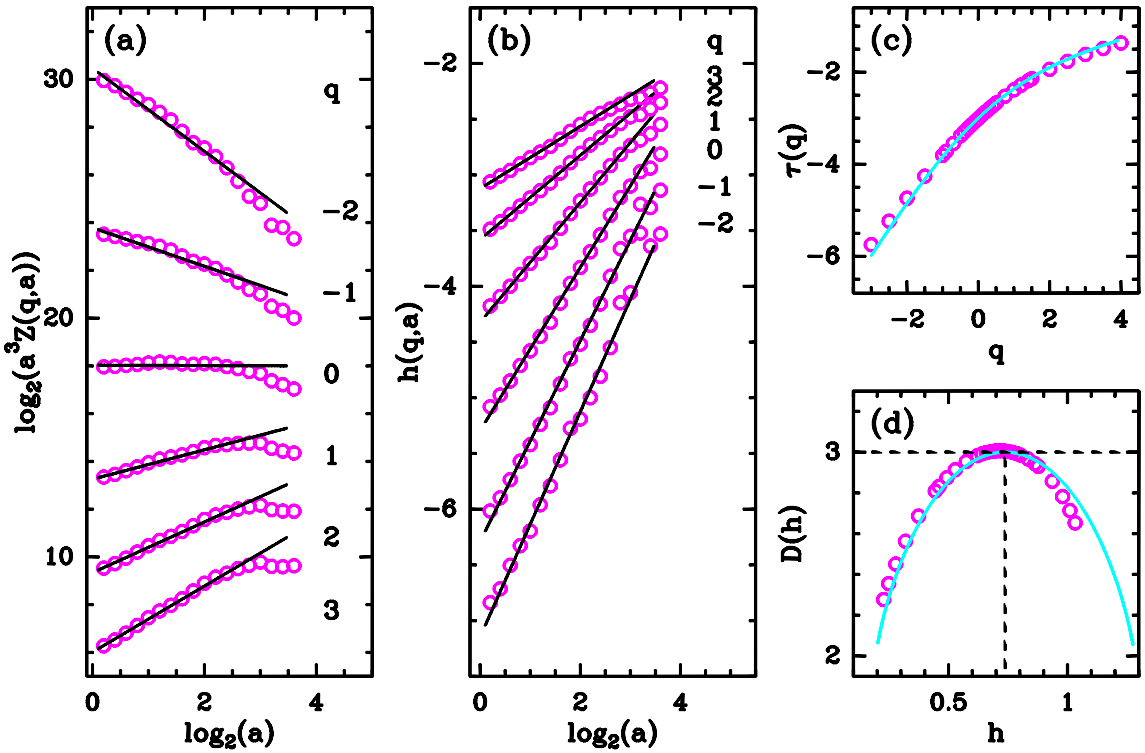

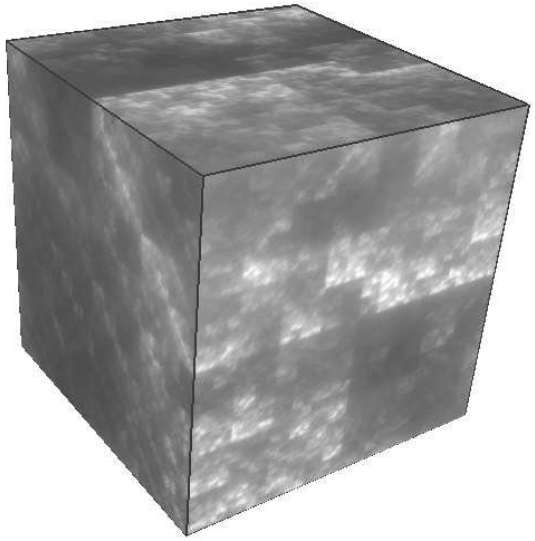

Theoretical predictions :

- $\tau(q) = -2 - q(1 - H^*) - \log_2(p_1{}^q + p_2{}^q)$. with $p_1 + p_2 = 1$
- **singularity spectrum is a non-degenerated convexe curve**

3D dissipation field : isotropic turbulence DNS

pseudo-spectral code, $(512)^3$ **grid,** $R_\lambda = 216$ **(M. Meneguzzi)**

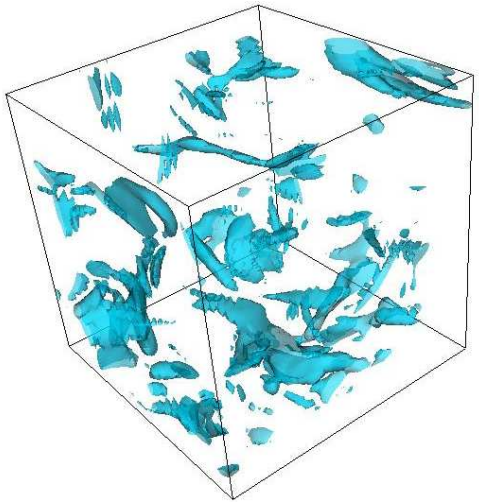

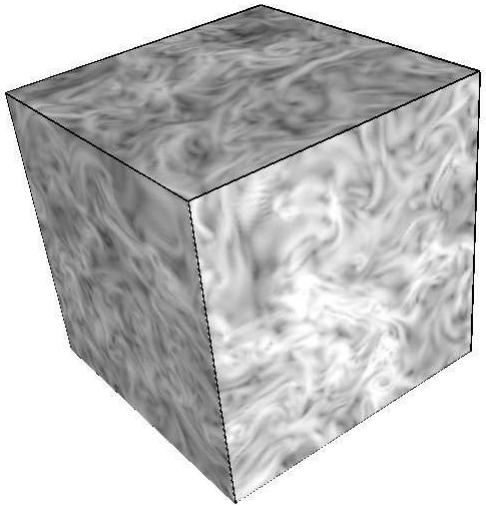

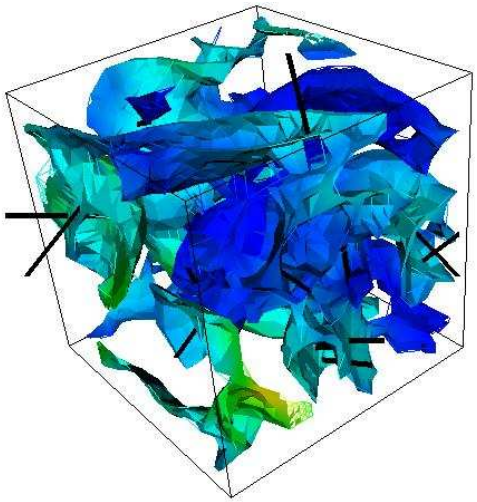

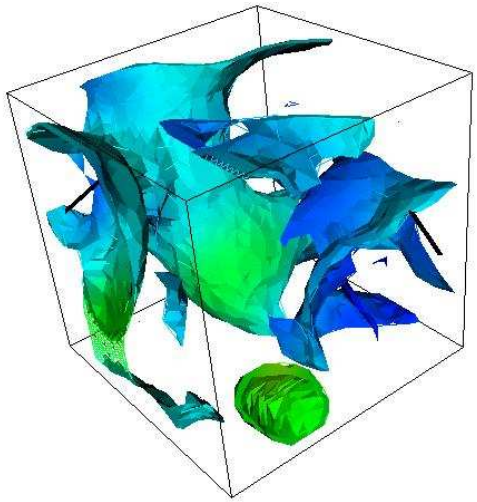

3D WTMM methodology *vs* Box-Counting algorithms

☞ "**Box-Counting**" algorithm, binomial fit with $p_1 = 0.3$ and $p_2 = 0.7 \rightarrow$ $\boxed{p_1 + p_2 = 1}$: diagnoses a **conservative** multiplicative structure

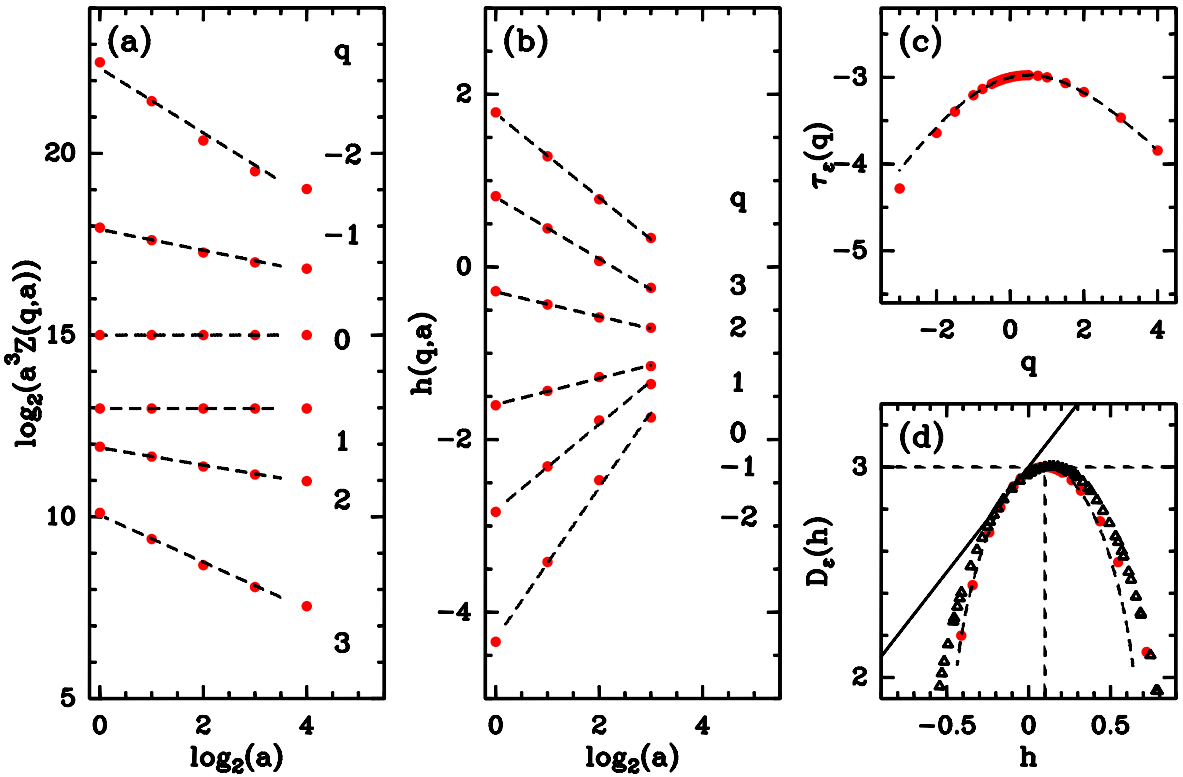

dissipation

binomial model :

$$\tau(q) = -2 - q - \log_2(p_1{}^q + p_2{}^q)$$

3D WTMM methodology *vs* Box-Counting algorithms

☞ "**Box-Counting**" algorithm, binomial fit with $p_1 = 0.3$ and $p_2 = 0.7 \rightarrow$ $\boxed{p_1 + p_2 = 1}$: diagnoses a **conservative** multiplicative structure

☞ "**3D WTMM**"method reveals a **non-conservative** multiplicative structure :

binomial fit with $p_1 = 0.36$ and $p_2 = 0.80 \Rightarrow$ $\boxed{p_1 + p_2 \neq 1}$

dissipation

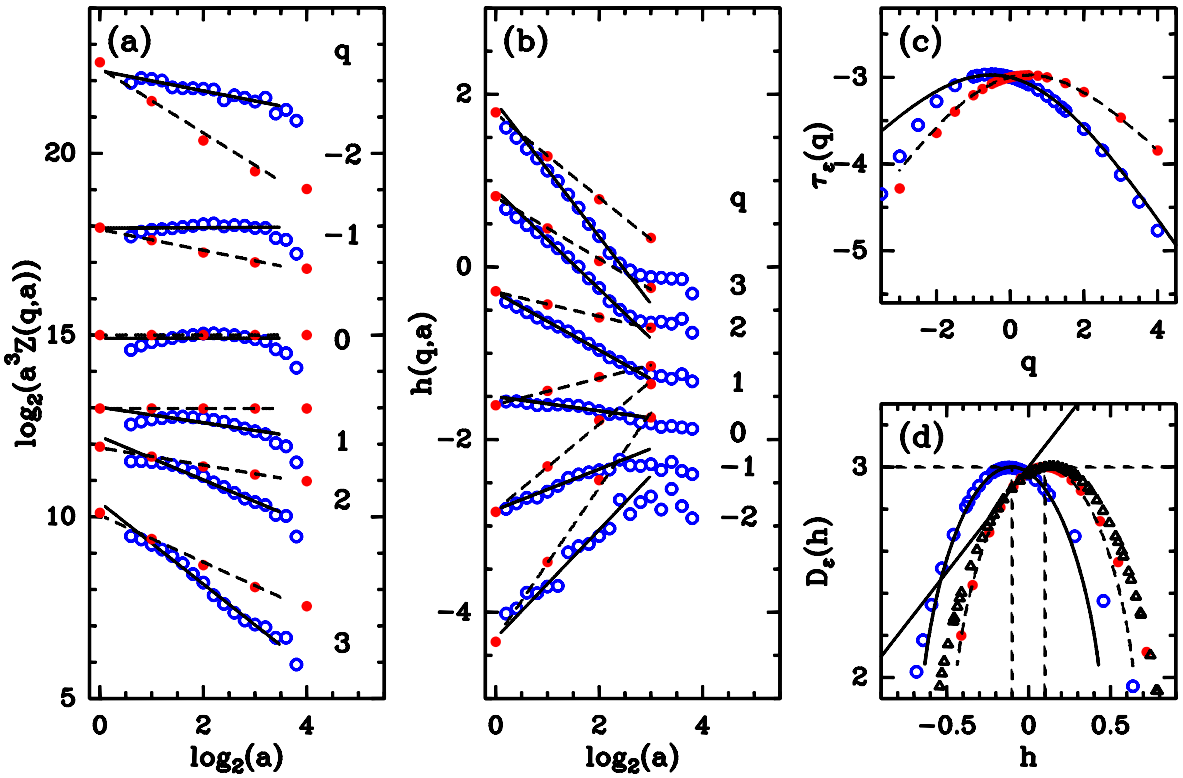

binomial model :

$$\tau(q) = -2 - q - \log_2(p_1{}^q + p_2{}^q)$$

remark:

$p_1 = \frac{p_1}{p_1 + p_2}$

$\Rightarrow$ inconsistent box-counting !

Comparative 3D WTMM analysis of dissipation and enstrophy

☞ **Dissipation, non-conservative multiplicative structure :**

binomial fit with $p_1 = 0.36$ **and** $p_2 = 0.80 \Rightarrow \boxed{p_1 + p_2 = 1.16}$

☞ **Enstrophy, non-conservative multiplicative structure :**

binomial fit with $p_1 = 0.38$ **and** $p_2 = 0.94 \Rightarrow \boxed{p_1 + p_2 = 1.32}$

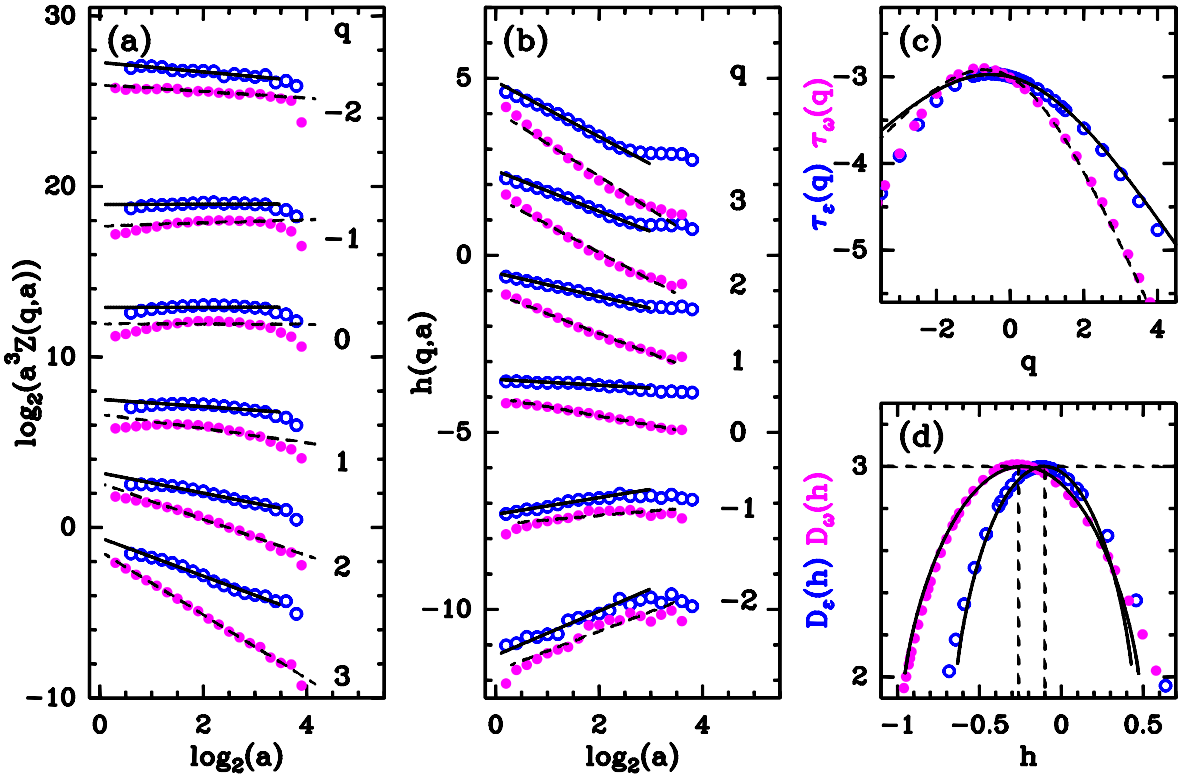

Intermittency coefficients:

- Dissipation : $C_2 \sim 0.22$
- Enstrophy : $C_2 \sim 0.30$

Self-similar multifractal vector-valued measure (2D case)

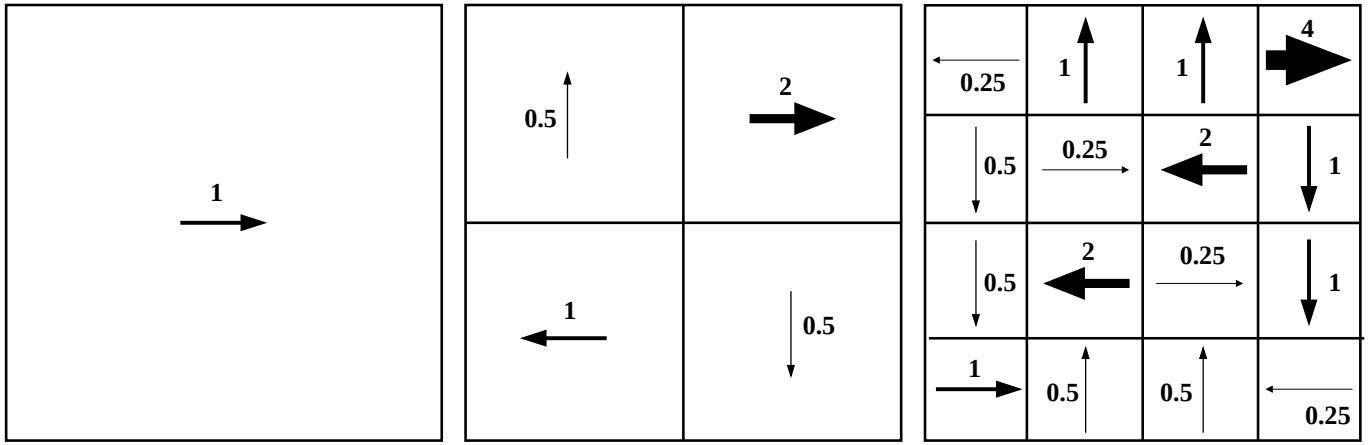

- **Falconer and O'Neil (1995)**
- **scalar measure** $\{\mathrm{r} : \lim_{l \to 0} \frac{\log \mu(B(\mathrm{r},l))}{\log l} = \alpha\}, \quad \alpha = h + 2$

  $\mathcal{Z}(q,l) = \sum_i \mu_i^q(l) \sim l^{\tau_\mu(q)}$
- **vector-valued measure** $\left\{\mathrm{r} : \lim_{l \to 0} \frac{\log \int_{B(\mathrm{r},l)} ||\Phi_l \mu(\mathrm{s})|| d\mathcal{L}_d(\mathrm{s})}{\log l} = \alpha\right\}, \quad \alpha = h + 2$

  $\mathcal{Z}(q,l) = \sum_i ||\Phi_l \mu||_i^q \sim l^{\tau_\mu(q)}$

Self-similar multifractal vector-valued measure (2D case)

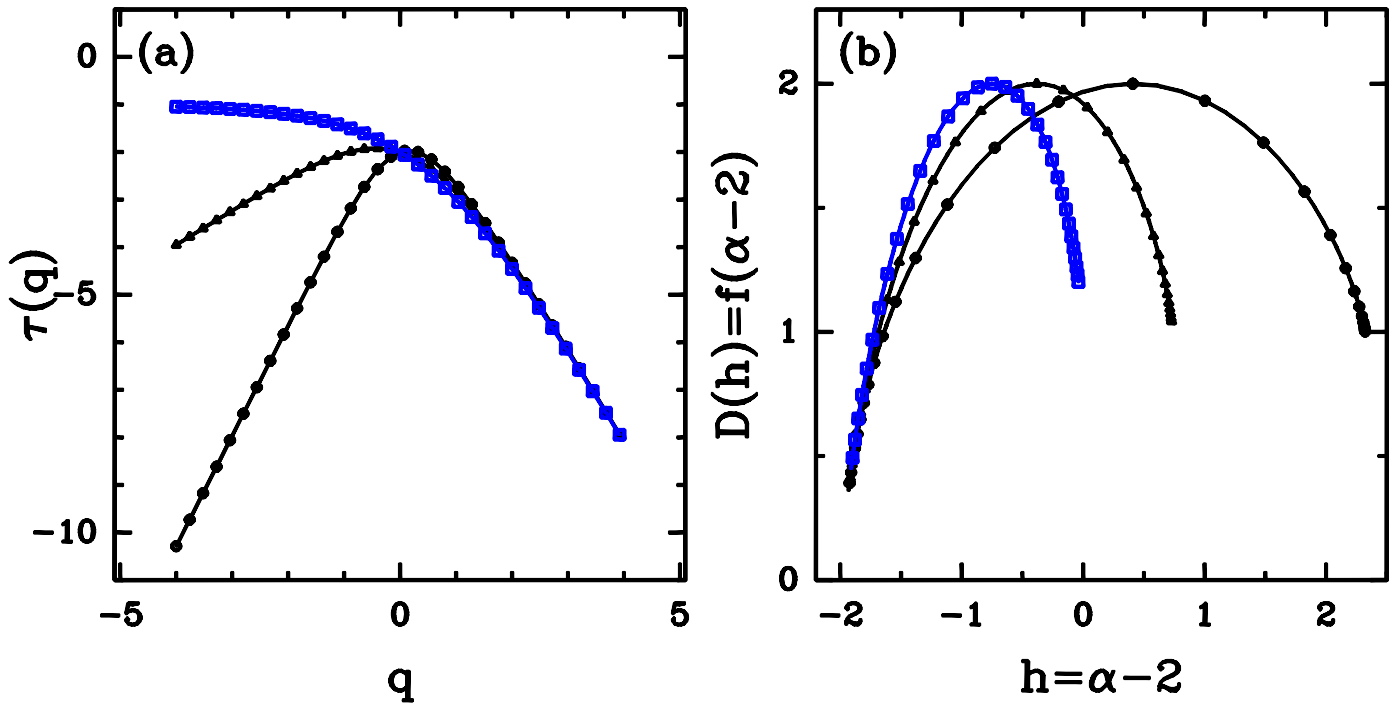

- $\tau_\mu(q) = -\frac{\log(p_1^q + p_2^q + p_3^q + p_4^q)}{\log 2}$
- $D_\mu(h) = f_\mu(\alpha - 2) = \inf_q(qh - \tau_\mu(q))$.

Tensorial wavelet transform (2D case)

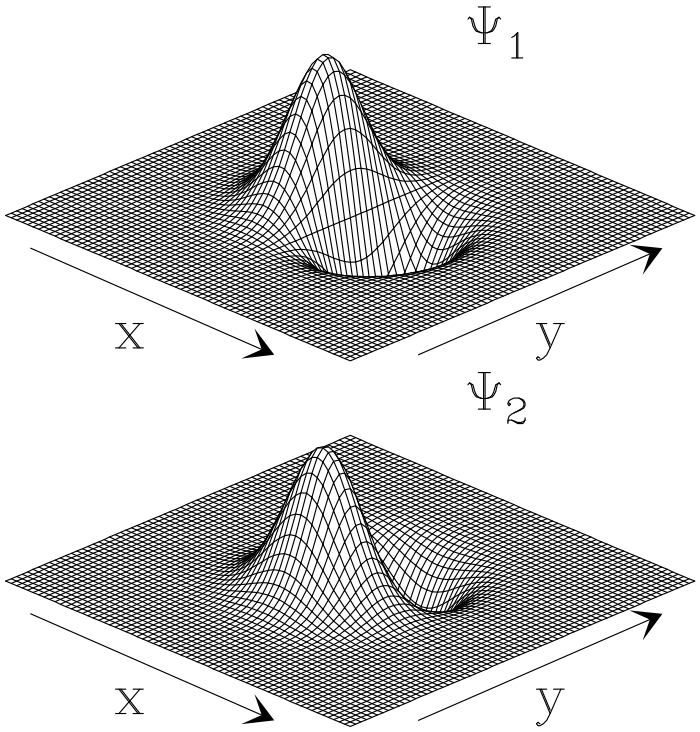

1. **Tensorial wavelet transform of field $\mathbf{V} = (V_1, V_2)$:**

$$\mathbb{T}_{\psi}[\mathbf{V}](\mathbf{b}, a) = (\mathbf{T}_{\psi_i}[V_j](\mathbf{b}, a)) = \begin{pmatrix} T_{\psi_1}[V_1] & T_{\psi_1}[V_2] \\ T_{\psi_2}[V_1] & T_{\psi_2}[V_2] \end{pmatrix}$$

$$T_{\psi_i}[V_j](\mathbf{b}, a) = a^{-2} \int d^2x\mathbf{r}\ \psi_i\left(a^{-1}(\mathbf{r} - \mathbf{b})\right) V_j(\mathbf{r}), j = 1, 2$$

2. **Direction of greatest variation of vector field :**

$$|\mathbb{T}_{\psi}[\mathbf{V}]| = \sup_{\mathbf{C} \neq \mathbf{0}} \frac{||\mathbb{T}_{\psi}[\mathbf{V}].\mathbf{C}||}{||\mathbf{C}||}$$

3. **Singular value decomposition of WT tensor:**

$$\mathbb{T}_{\psi}[\mathbf{V}] = \left(G\right).\begin{pmatrix} \sigma_{\max} & 0 \\ 0 & \sigma_{\min} \end{pmatrix}.\left(D\right)^T$$

4. **Tensorial wavelet transform** :

$$\mathbf{T}_{\psi,\max}[\mathbf{V}](\mathbf{b}, a) = \sigma_{\max}\mathbf{G}_{\sigma_{\max}}$$

Tensorial 2D WTMM methodology

Data

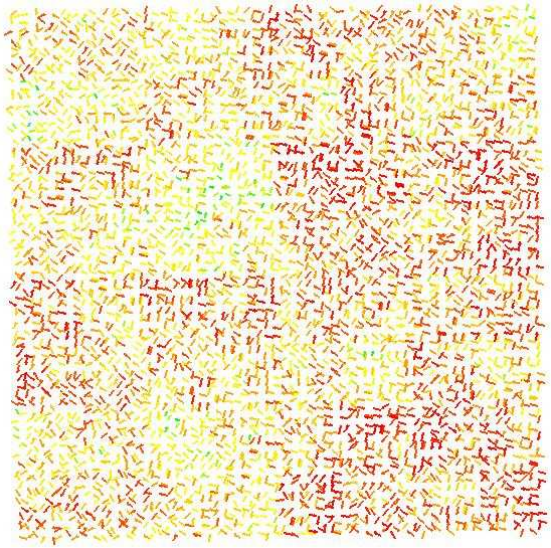

Tensorial wavelet transform

$$\mathbf{T}_{\boldsymbol{\psi},\max}[\mathbf{V}](\mathbf{b}, a) = \sigma_{\max}\mathbf{G}_{\sigma_{\max}}$$

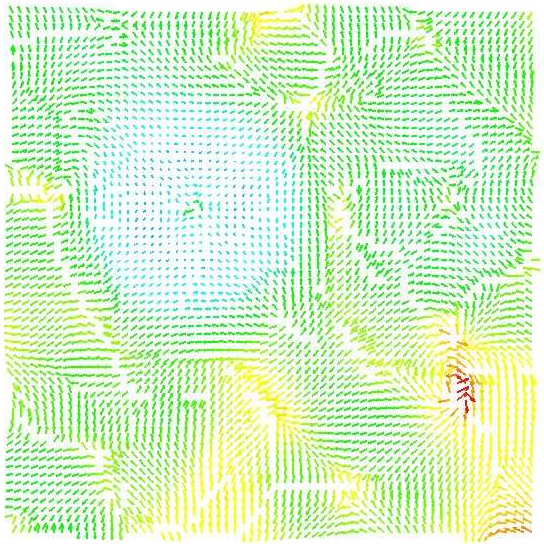

Modulus Maxima $\boldsymbol{\sigma_{\max}}$ chains of tensorial wavelet transform at scale a :

$$\left\{(b, a)/\frac{\partial \sigma_{\max}}{\partial G_{\max}} = 0 \quad \text{et} \quad \frac{\partial^2 \sigma_{\max}}{\partial G_{\max}^2} < 0\right\}$$

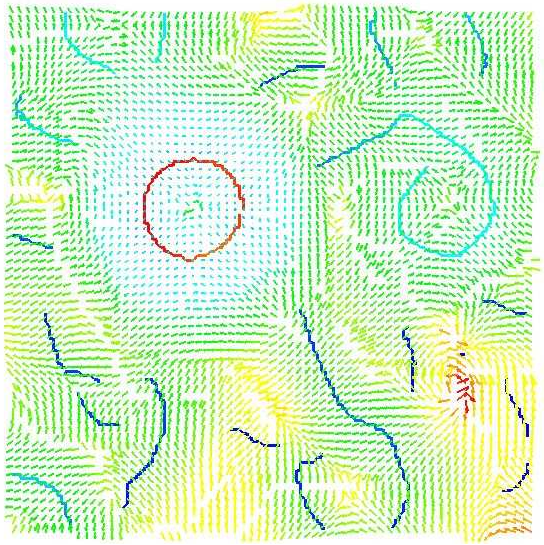

Tensorial 2D WTMM methodology: Skeleton

WTMM Chains

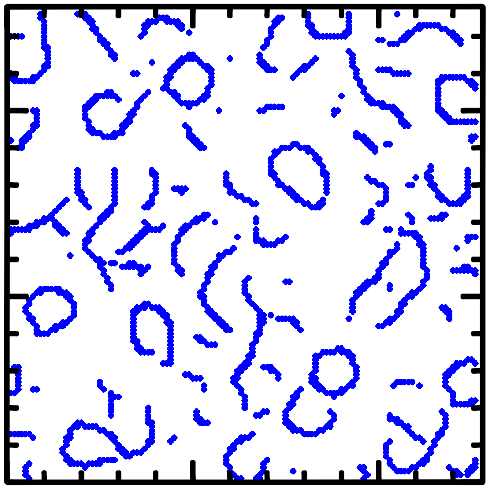

WTMMM

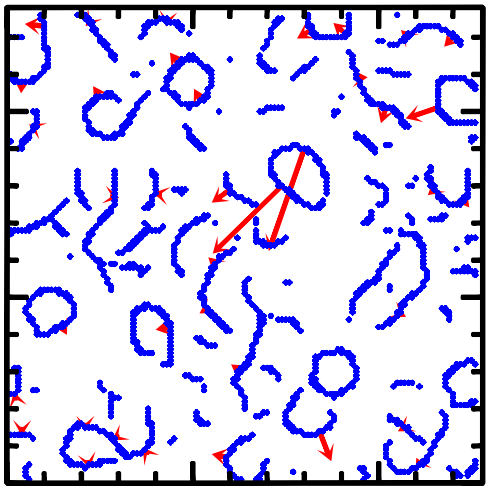

WTMM Chains at 3 different scales

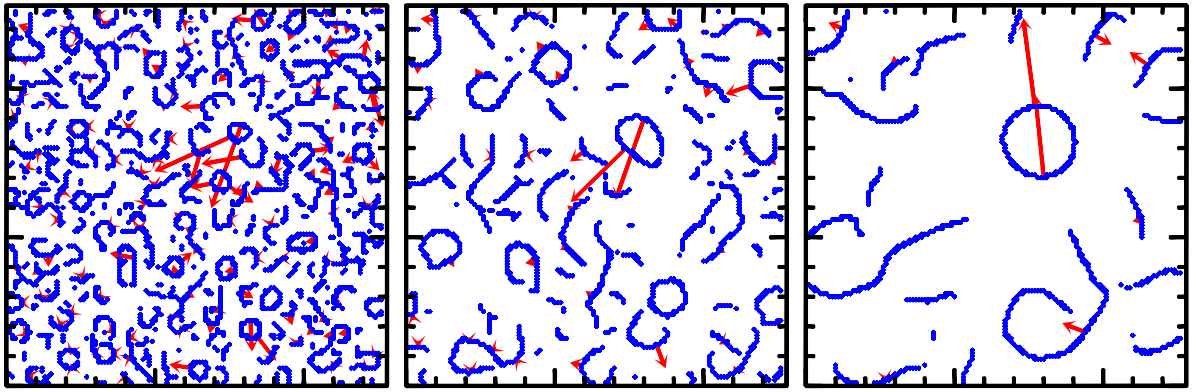

WTMMM linking: WT Skeleton

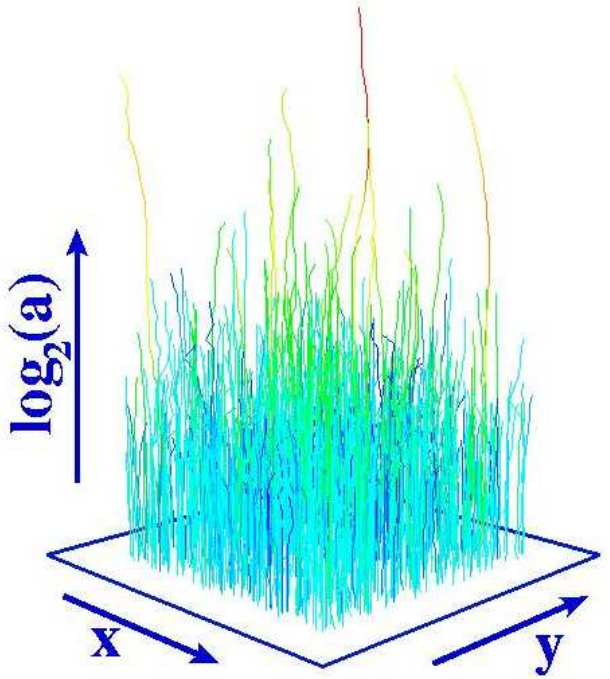

Monofractal 2D vector fields

fractional Brownian fields : $\mathrm{B}_H(\mathrm{r})$

☞ **Spectral method simulation**

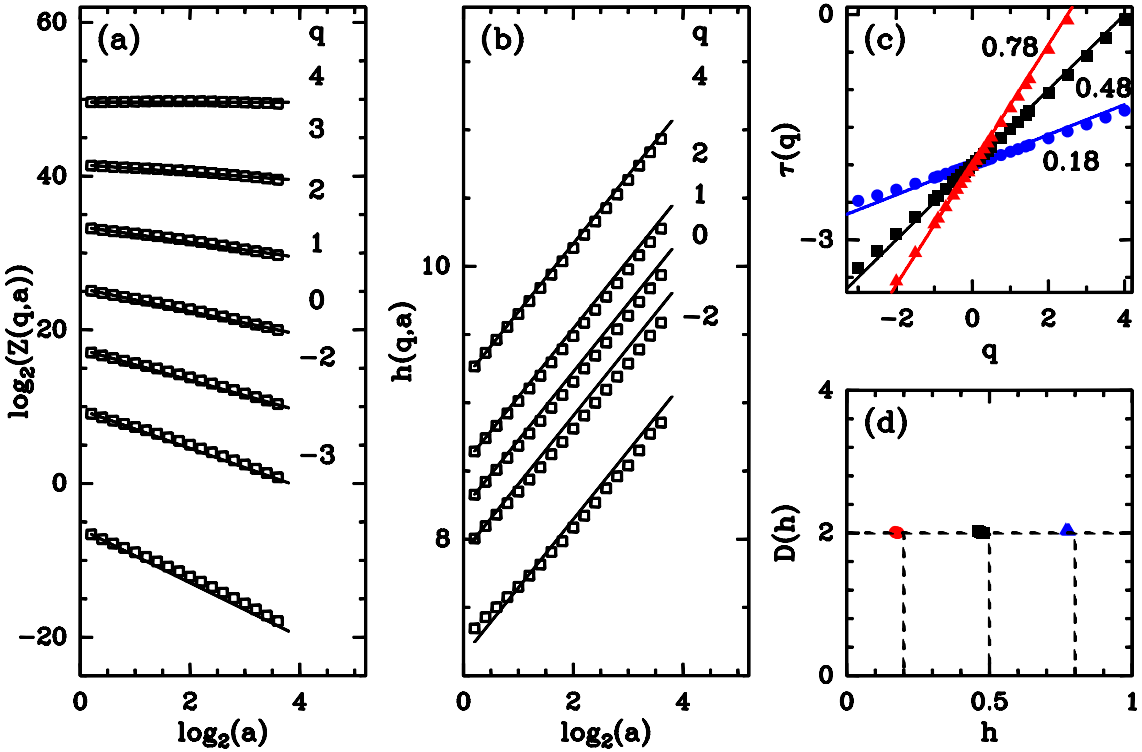

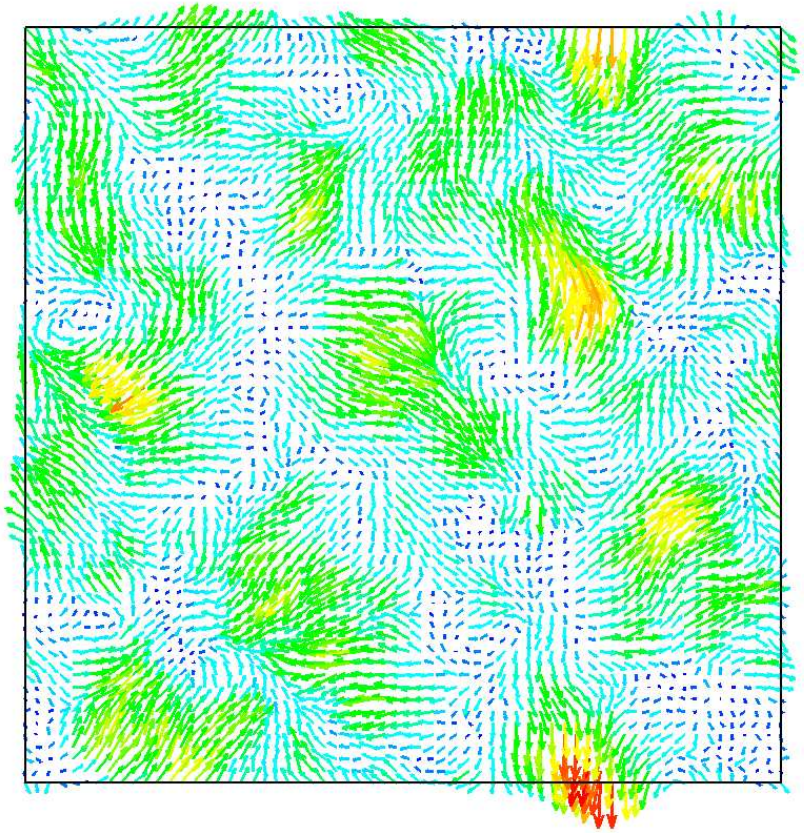

Theoretical predictions :

- linear $\tau(q)$: $\tau(q) = qH - 2$
- degenerated singularity spectrum:

$$D(h = H) = 2$$

2D self-similar multifractal vector-valued measures

Self-similar multifractal vector-valued measures (Falconer and O'Neil's model)

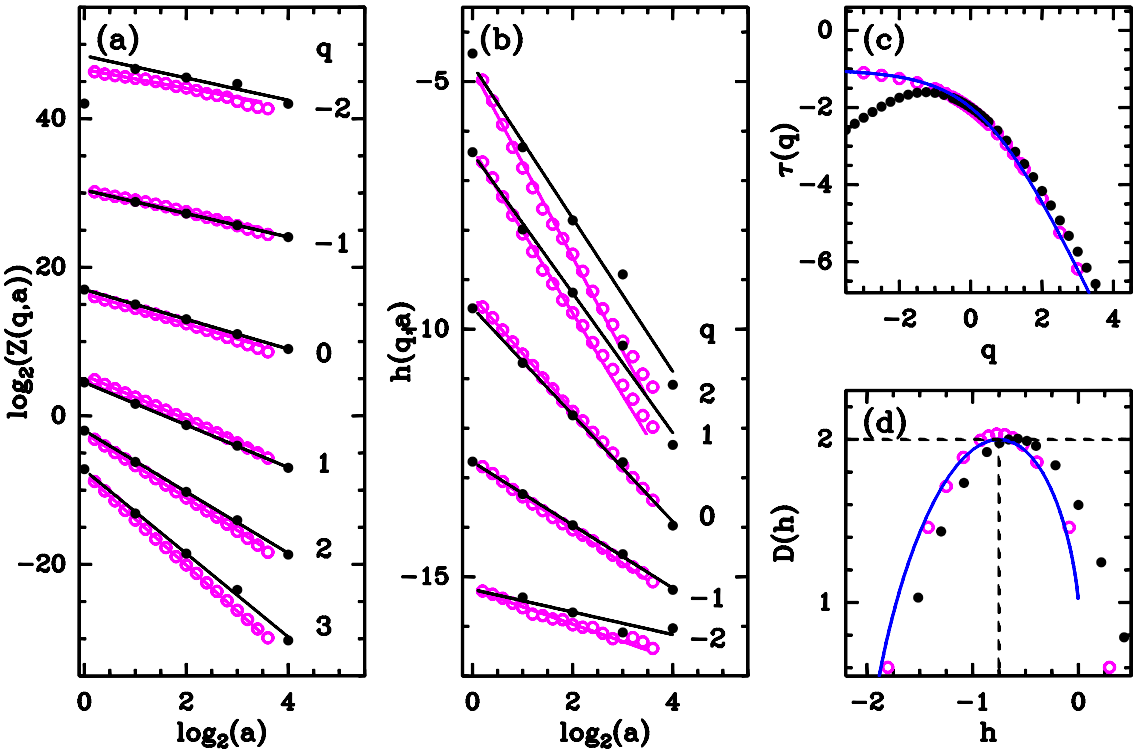

- vectorial box-counting
- vectorial 2D WTMM method

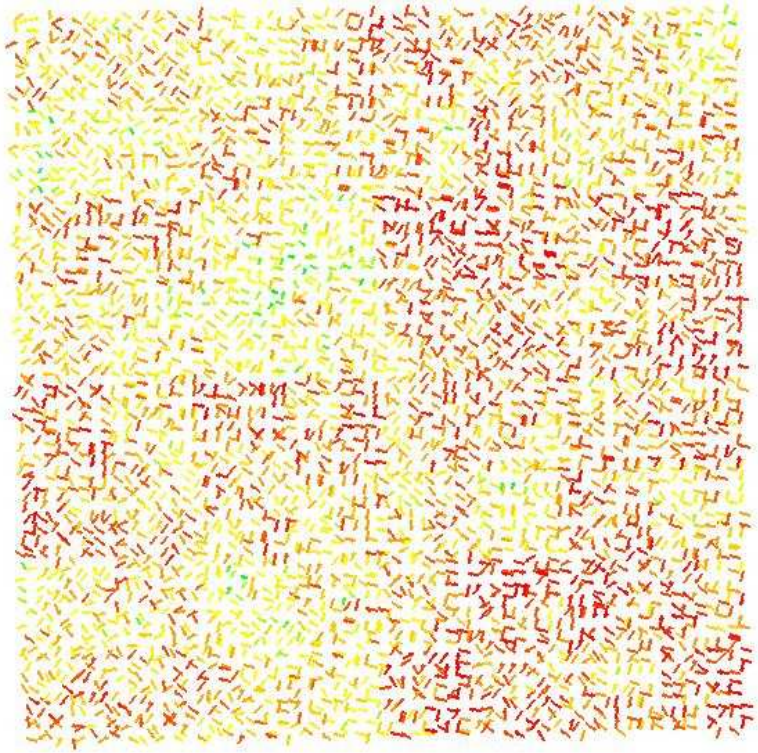

Theoretical predictions:

- $\tau(q) = -\log_2(p_1{}^q + p_2{}^q + p_3{}^q + p_4{}^q)$
  $p_1 = p_4 = 0.5$, $p_2 = 2$ and $p_3 = 1$
- **vectorial box-counting is less accurate**

Tensorial 3D WTMM method: turbulent velocity field ($R_\lambda = 140$)

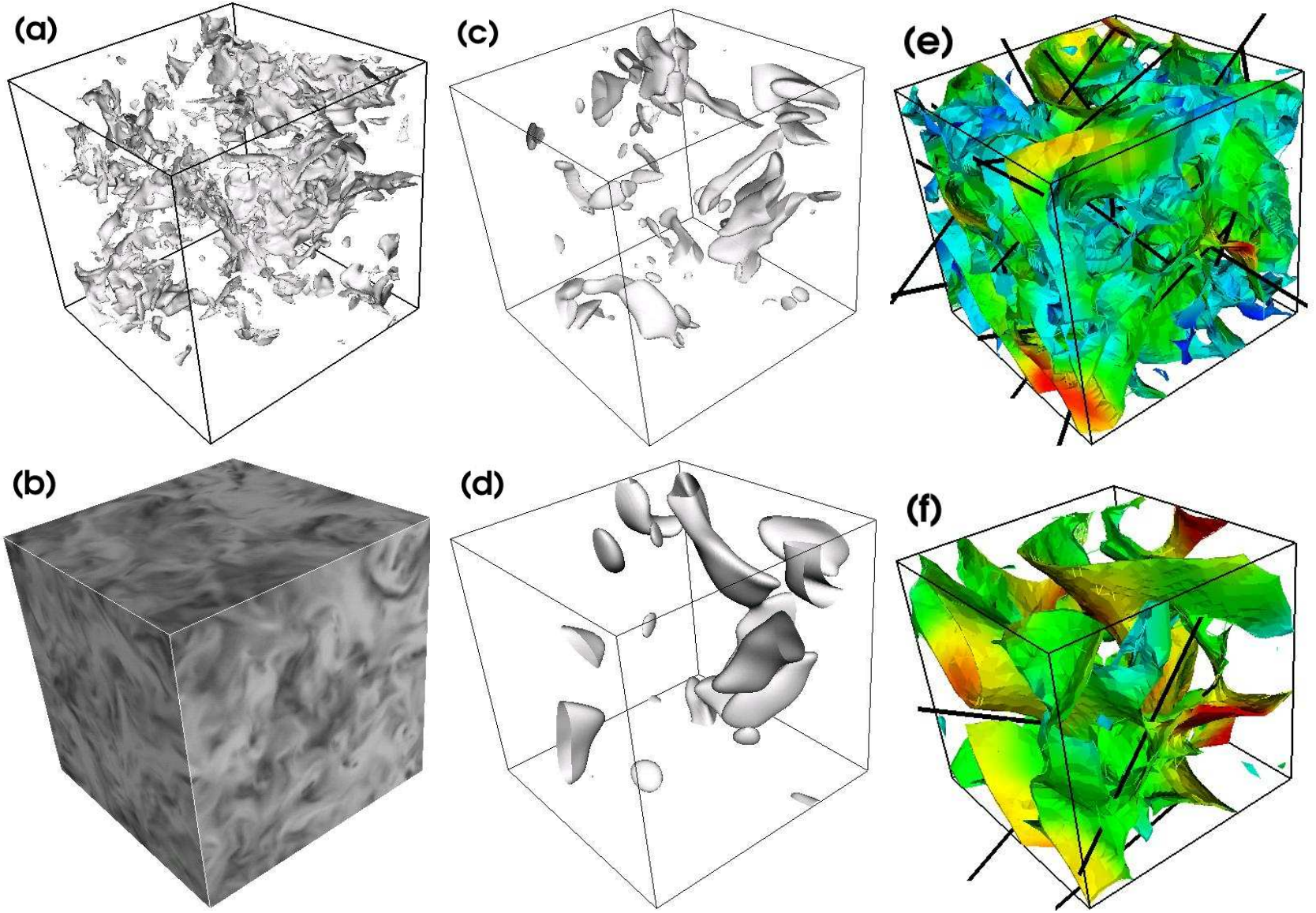

Tensorial 3D WTMM method: singularity spectrum of velocity

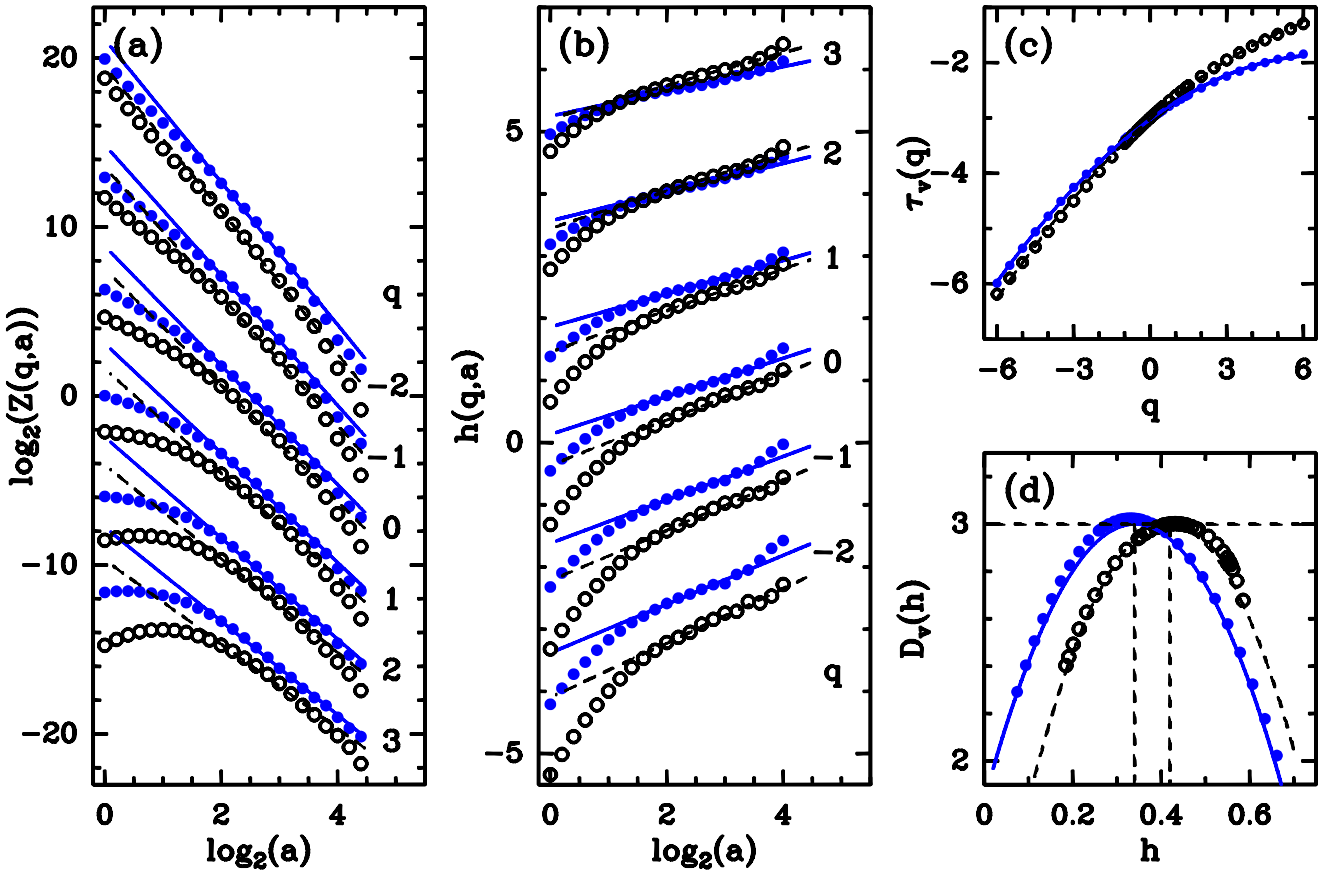

- parabolic fi t : $\tau(q) = -C_0 - C_1 q - C_2 \frac{q^2}{2}$
- intermittency coeffi cient $C_2 = 0.049 \pm 0.004$

1D increments method:

- longitudinal : $C_2(\delta v_L) \sim 0.025$
- transverse : $C_2(\delta v_T) \sim 0.040$

Tensorial 3D WTMM method: turbulent velocity field ($R_\lambda = 140$)

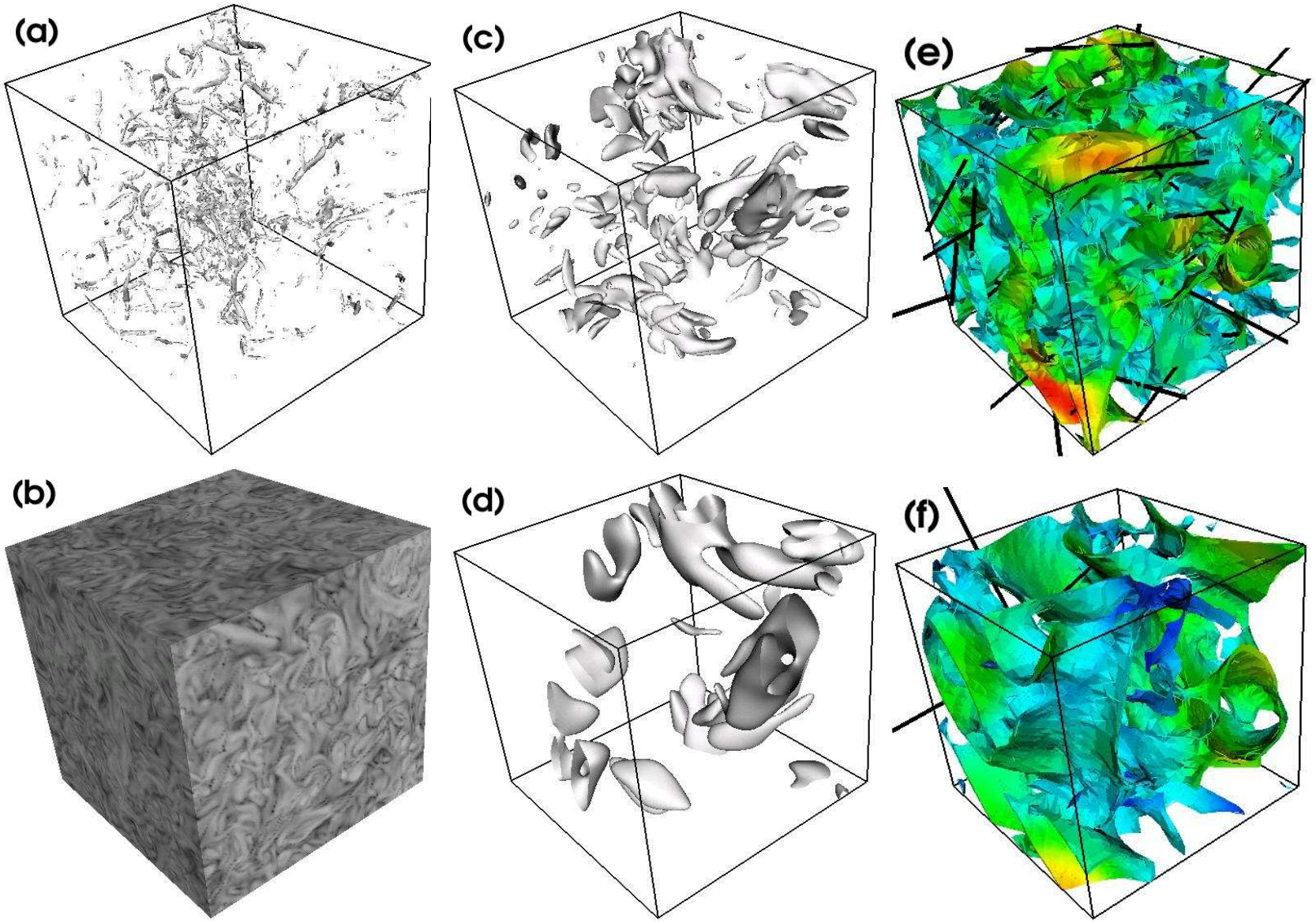

Tensorial 3D WTMM method: singularity spectrum of vorticity

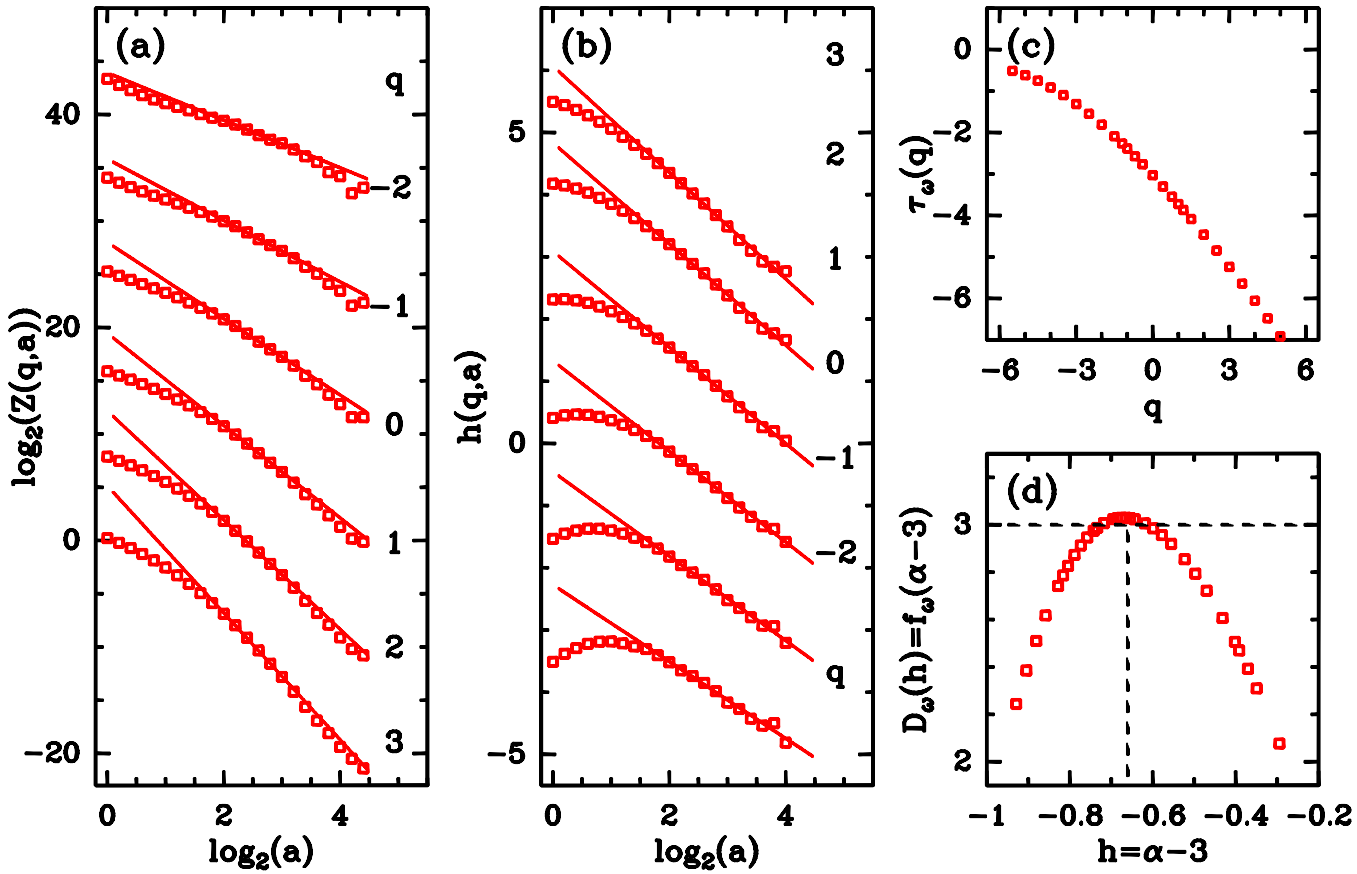

- vorticity

Tensorial 3D WTMM method: singularity spectrum of vorticity

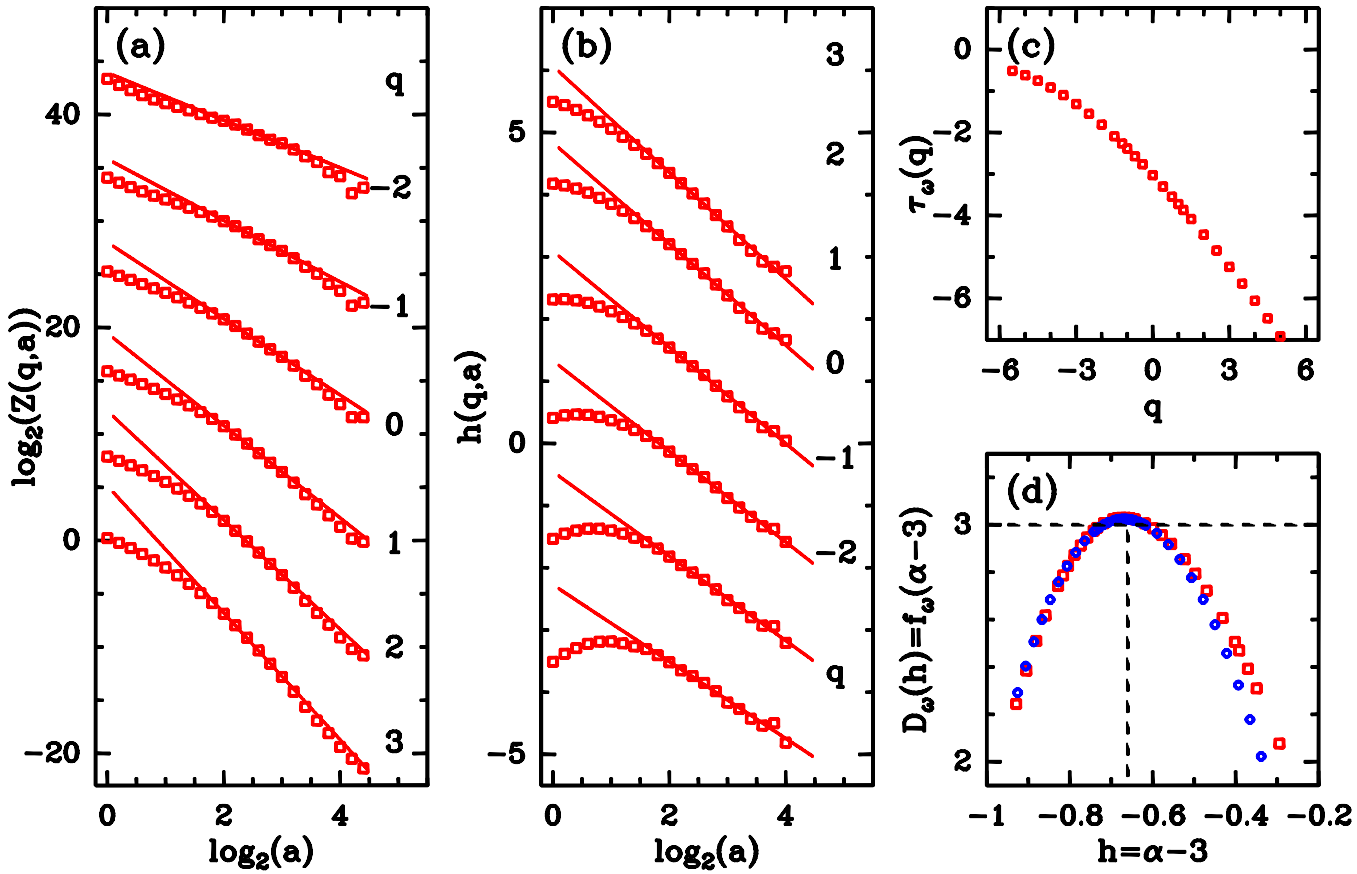

□ vorticity

∘ $D_v(h+1)$ spectrum translated velocity

$\Rightarrow$ same 3D intermittency coefficient !

Conclusion

assessment:

- **WTMM multifractal analysis: moving towards vector fields**

outlooks :

- **better understanding of the information embedded in the WT tensor.**
- **identification of coherent structures in turbulence using WT tensor's smallest singular value: vorticity filaments or sheets.**
- **others applications : astrophysics (interstellar medium, interstellar turbulence), MHD, geophysics, ...**

Thanks :

- **E. Lévêque, Laboratoire de Physique, ENS Lyon (Turbulent flows DNS).**

References :

- **P. Kestener and A. Arneodo,** *Phys. Rev. Lett.*, **91:194501, 2003.**
- **P. Kestener and A. Arneodo,** *Phys. Rev. Lett.*, **93:044501, 2004.**

Preliminary results :

Isosurface plots of data and 3D WT modulus (Gaussian filtering) :

$z = 5$ $z = 2$ $z = 0$

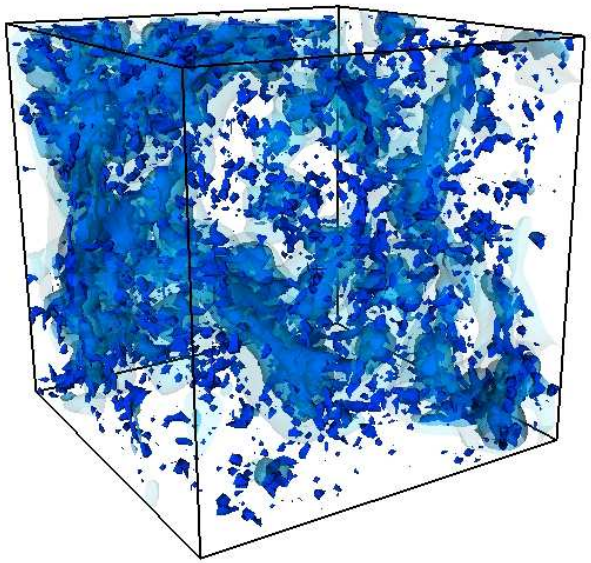

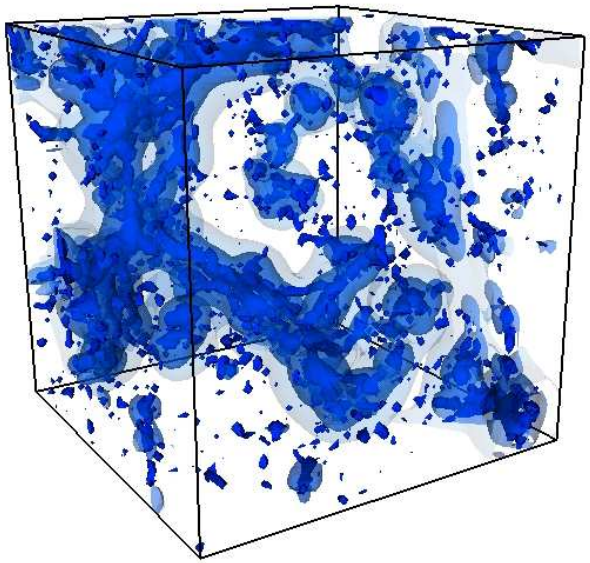

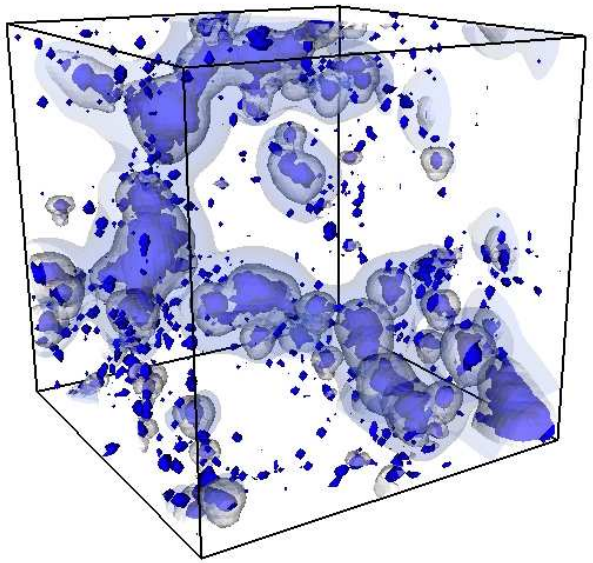

3D Box-Counting method: singularity spectrum ($z = 0$ and $z = 5$)

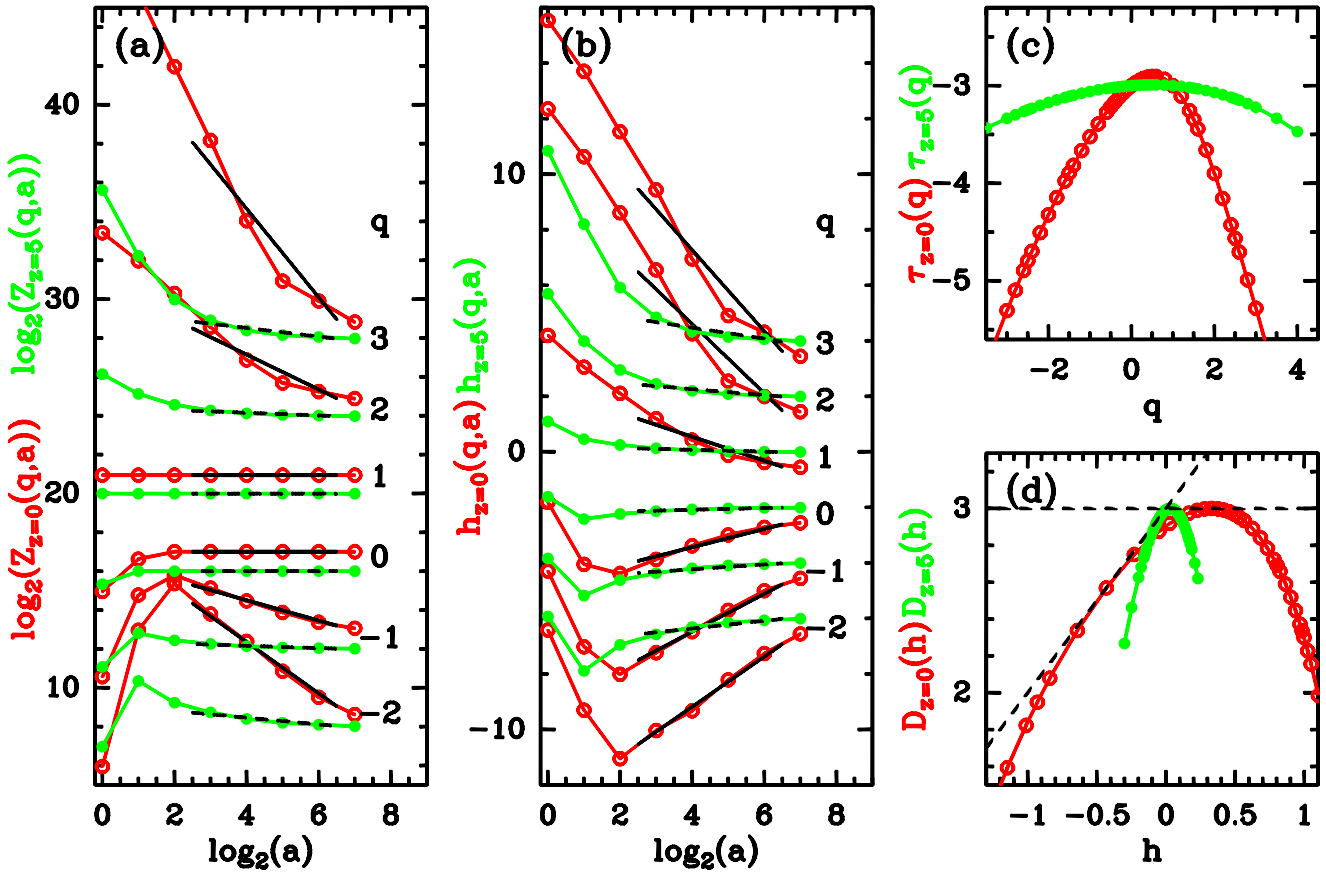

- NO CLEAR SCALING !!!
- perhaps scaling at large scales ??

Scalar 3D WTMM method: singularity spectrum ($z = 0$ and $z = 5$)

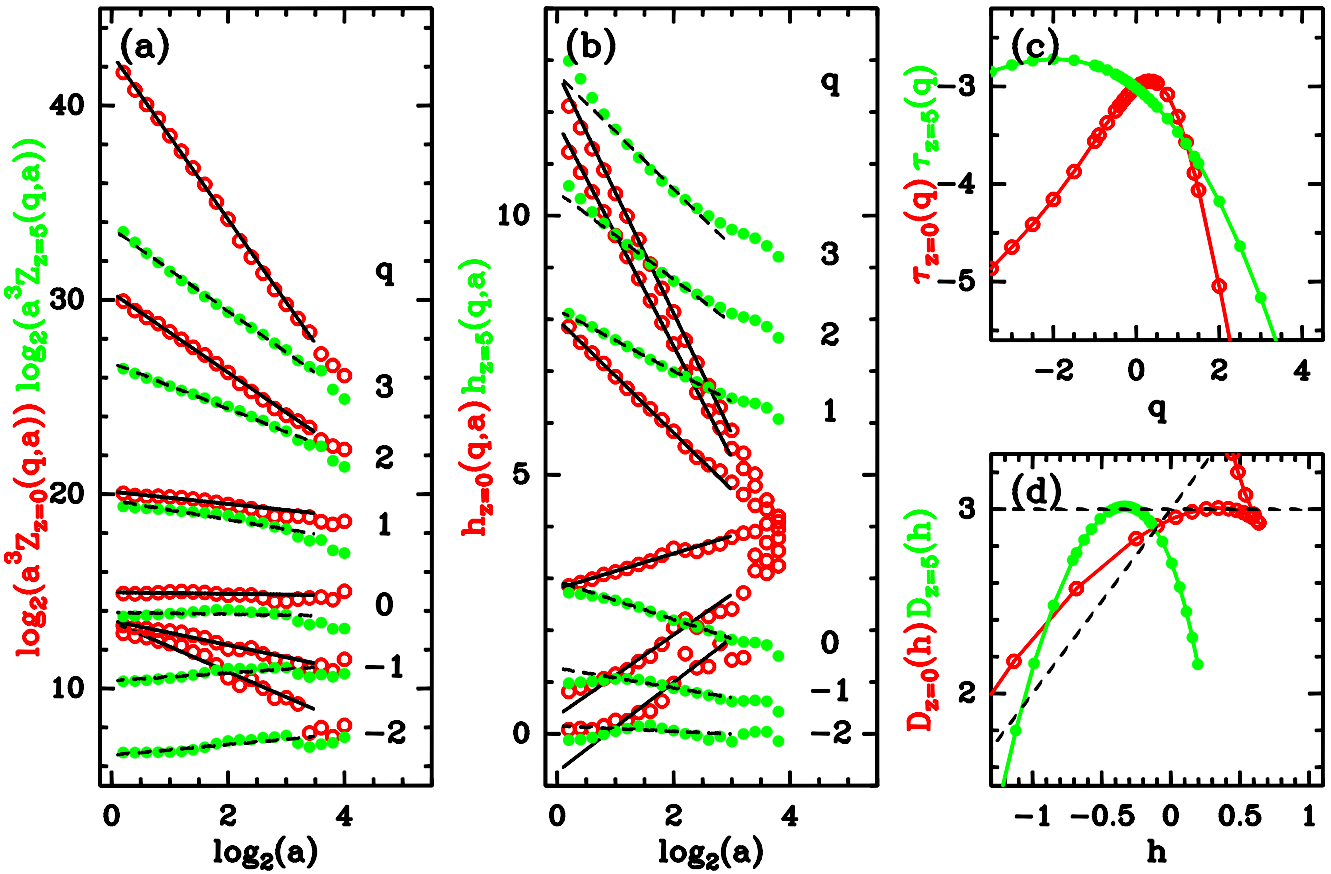

- parabolic fi t : $\tau(q) = -C_0 - C_1 q - C_2 \frac{q^2}{2}$
- intermittency coeffi cients $C_2 = 1.32 \pm 0.05$ $C_2 = 0.22 \pm 0.02$

Scalar 3D WTMM method: singularity spectra of galaxy distribution

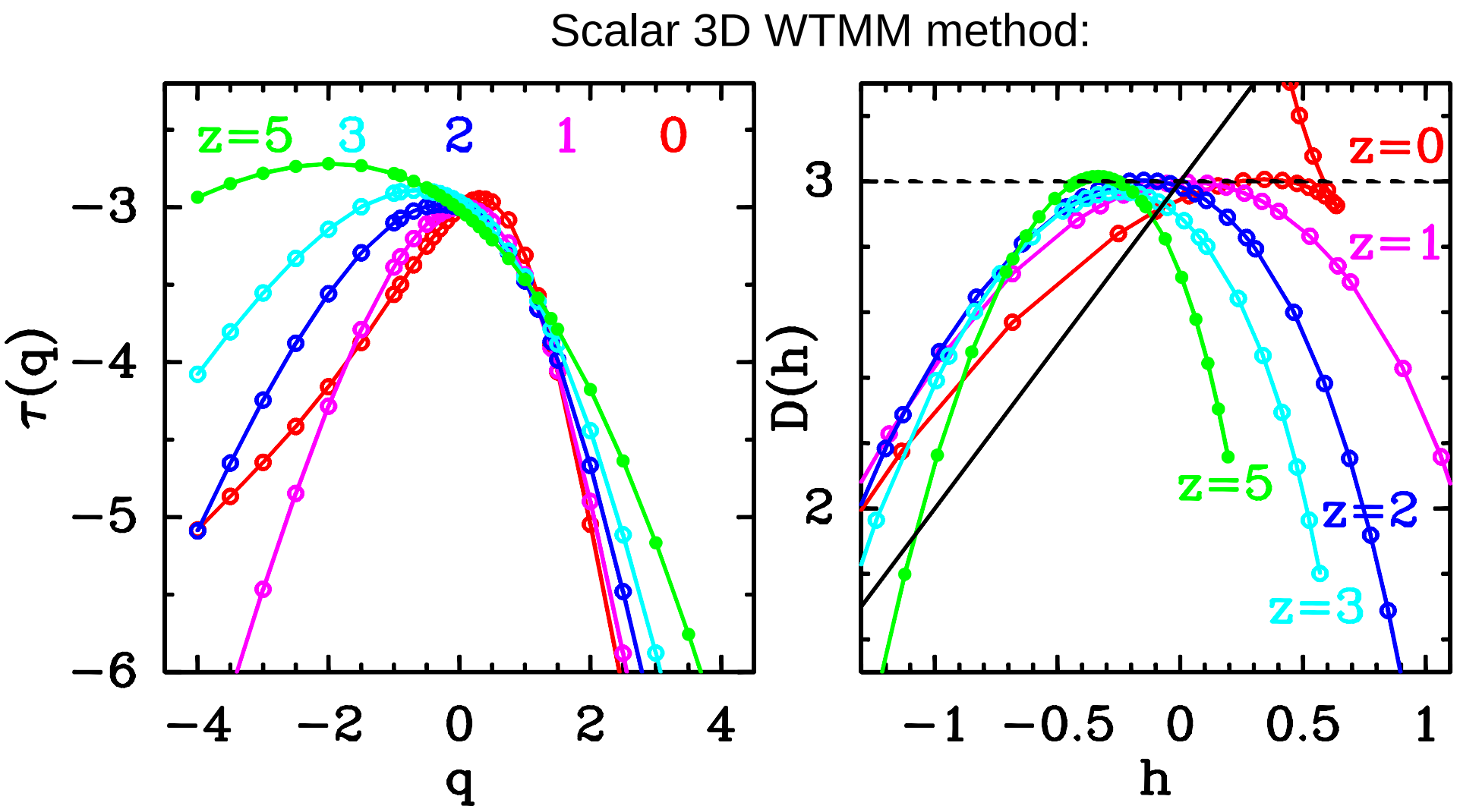

Box-Counting method: singularity spectra of galaxy distribution

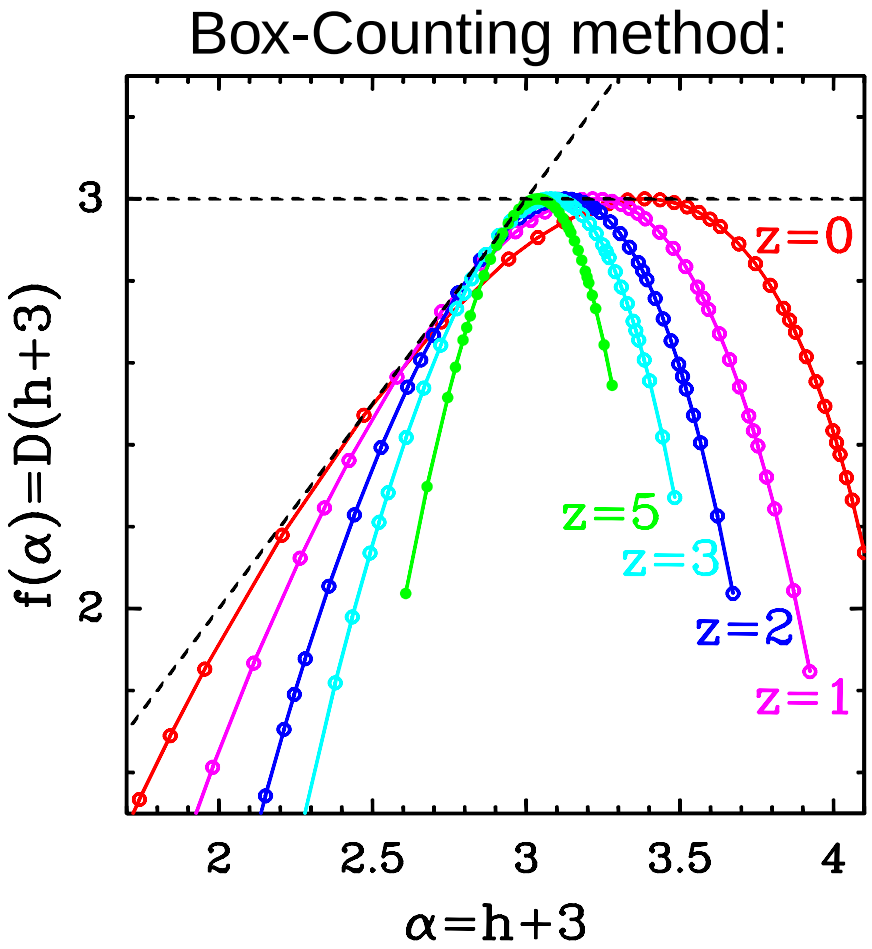

- Box-counting intermittency coefficients are smaller than those computed using 3D WTMM method !!! (To be continued).

Cancellation exponent basics

- **Signed singular measure :**
  $\forall A, \exists B \subset A / \ \mu_s(A)\mu_s(B) < 0$
  (ex : magnetic field component, ...)

- ***Cancellation exponent*** **:** $\kappa = \lim_{\varepsilon \to 0} \frac{\ln \sum_i |\mu(I_{i,\varepsilon})|}{\ln(1/\varepsilon)}$,
  where $\{I_{i,\varepsilon}\}$ **is a tiling of measure's support.**

- **using the wavelet transform:**
  $$\kappa = -D_F - \tau(q=1)$$
  $\Rightarrow$ **choice of the analyzing wavelet.**

- **link to the notion of conservativity of a multiplicative cascade:**
  $\kappa = -D_F - \tau(q=1) = \frac{\ln < M >}{\ln b}$ **: transfert rate of the measure from scale** a **to scale** a/b

- **conservative cascade** $\iff \kappa = 0$
  non-conservative cascade $\iff \kappa \neq 0$

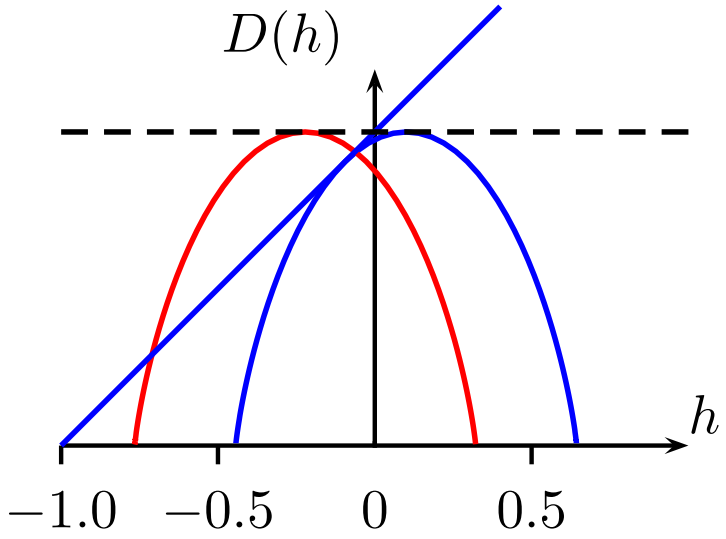

Recursive filter technics in 3D

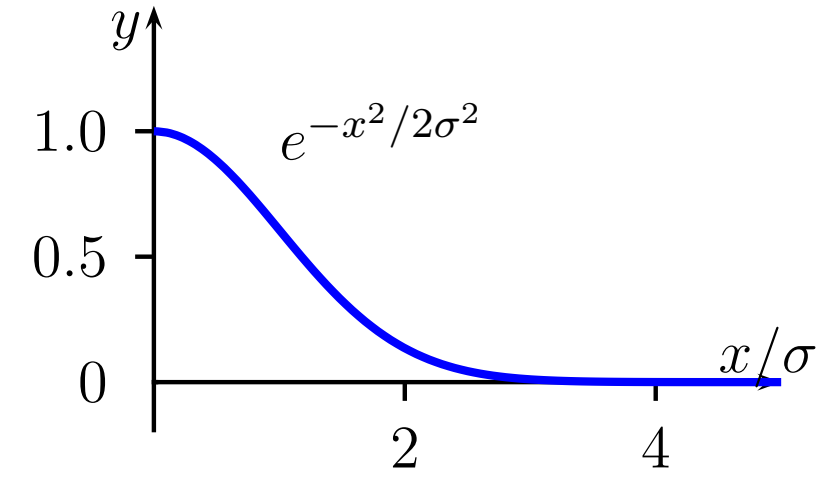

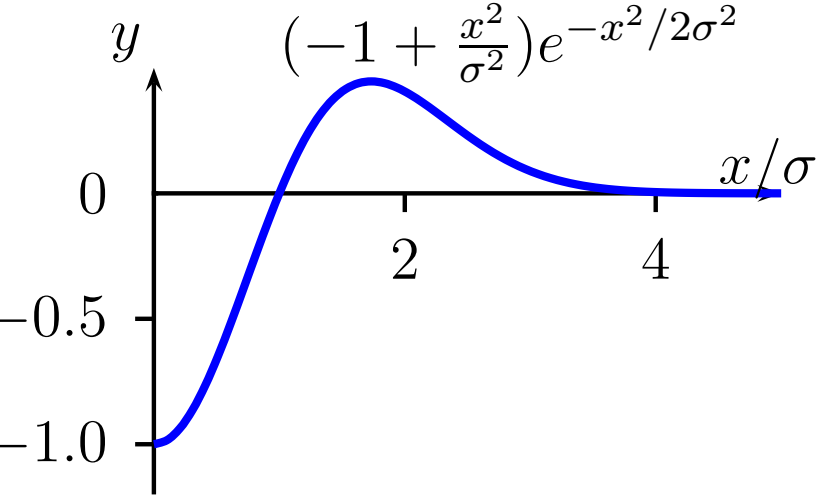

- Gaussian filter $e^{-x^2/2\sigma^2}$ approximated by $h_\sigma(x)$

$$(a_0\cos(\omega_0\tfrac{x}{\sigma})+a_1\sin(\omega_0\tfrac{x}{\sigma}))\exp^{-b_0\frac{x}{\sigma}}$$
$$+(c_0\cos(\omega_1\tfrac{x}{\sigma})+c_1\sin(\omega_1\tfrac{x}{\sigma}))\exp^{-b_1\frac{x}{\sigma}}$$

- Coefficients a_i, b_i, c_i and ω_i are estimated by minimizing the relative quadratic error:

$$\epsilon^2 = \frac{\sum_{i=1}^{10\sigma}(g_\sigma(i)-h_\sigma(i))^2}{\sum_{i=1}^{10\sigma} g_\sigma(i)^2}$$

- 4th order recursive equation:

$$y_k = n_{00}x_k + n_{11}x_{k-1} + n_{22}x_{k-2} + n_{33}x_{k-3} - d_{11}y_{k-1} - d_{22}y_{k-2} - d_{33}y_{k-3} - d_{44}y_{k-4}$$

- computing time decrease in 3D: 60 % for Gaussian filter and 25 % for Mexican filter

Box-counting algorithms : multifractal measure

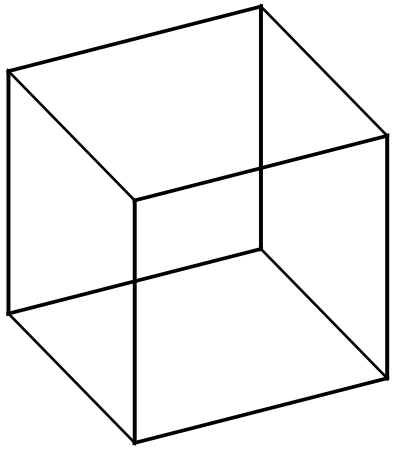
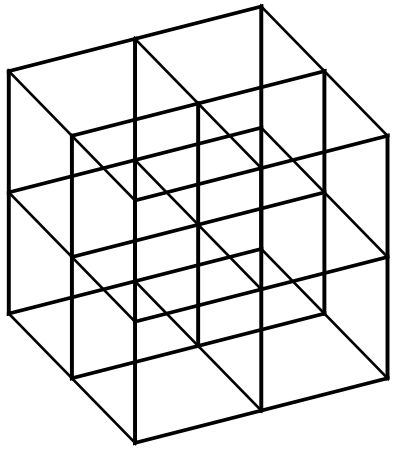
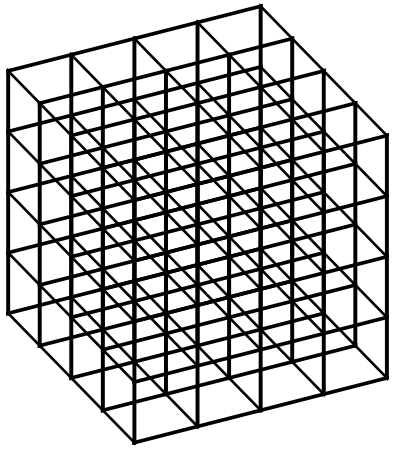

- μ: probability measure whose support $E \subset \mathbb{R}^d$
- singularity exponent: $\alpha(x) = \lim_{l \to 0} \frac{\log \mu(\mathcal{B}(l,x))}{\log l}$
- method: tile support of the measure with boxes of size $l_i = L/2^i$
- partition functions: $S_q(l_i) = \sum_{\mu(\mathcal{B}) \neq 0} \left[\mu(\mathcal{B})\right]^q =< \mu^q >$

  multifractal spectrum: $\tau(q) = \lim_{l \to 0} \frac{\log S_q(l)}{\log l}$;

$$f(\alpha) = D(h = \alpha - d) = \min_q(\alpha q - dq - \tau(q))$$

Singularity spectra of velocity and vorticity

To each velocity $\mathbf{v}$ field singularity $h(\mathbf{r}_0)$ corresponds a vorticity $\boldsymbol{\omega} = \boldsymbol{\nabla} \wedge \mathbf{v}$ singularity $h(\mathbf{r}_0) - 1$:

$$\mathbf{f}(\mathbf{x_0}+\mathbf{l}) = \mathbf{f}(\mathbf{x_0}) + (\boldsymbol{\nabla}_\mathbf{x})\mathbf{f}(\mathbf{x_0})\mathbf{l} + \ldots + (\boldsymbol{\nabla}_\mathbf{x})^n \mathbf{f}(\mathbf{x_0})\mathbf{l}^{(n)} + |\mathbf{l}|^{h(\mathbf{x_0})}\mathbf{C}(\mathbf{l})$$

$$\boldsymbol{\nabla}_\mathbf{x} \wedge \mathbf{f}(\mathbf{x_0}+\mathbf{l}) = \boldsymbol{\nabla}_\mathbf{x} \wedge \mathbf{f}(\mathbf{x_0}) + \boldsymbol{\nabla}_\mathbf{x} (\boldsymbol{\nabla}_\mathbf{x} \wedge \mathbf{f})(\mathbf{x_0})\mathbf{l} + \ldots + \boldsymbol{\nabla}_\mathbf{x}^{n-1} (\boldsymbol{\nabla}_\mathbf{x} \wedge \mathbf{f})(\mathbf{x_0})\mathbf{l}^{(n-1)} + h|\mathbf{l}|^{h-1}\mathbf{u}_\mathbf{l} \wedge \mathbf{C}(\mathbf{l})$$

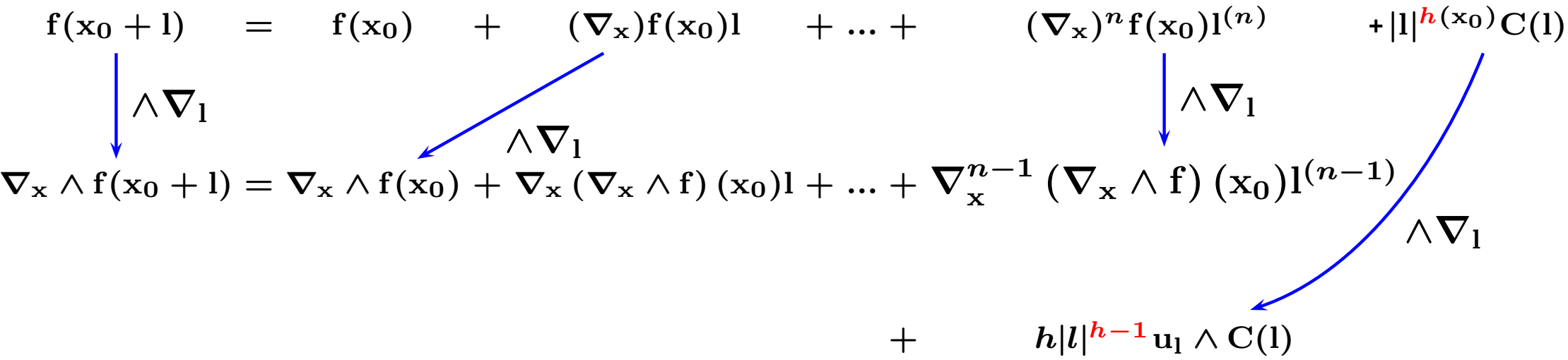

Mammography and breast anatomy

Goals : using WTMM method to diagnosis help of breast cancer

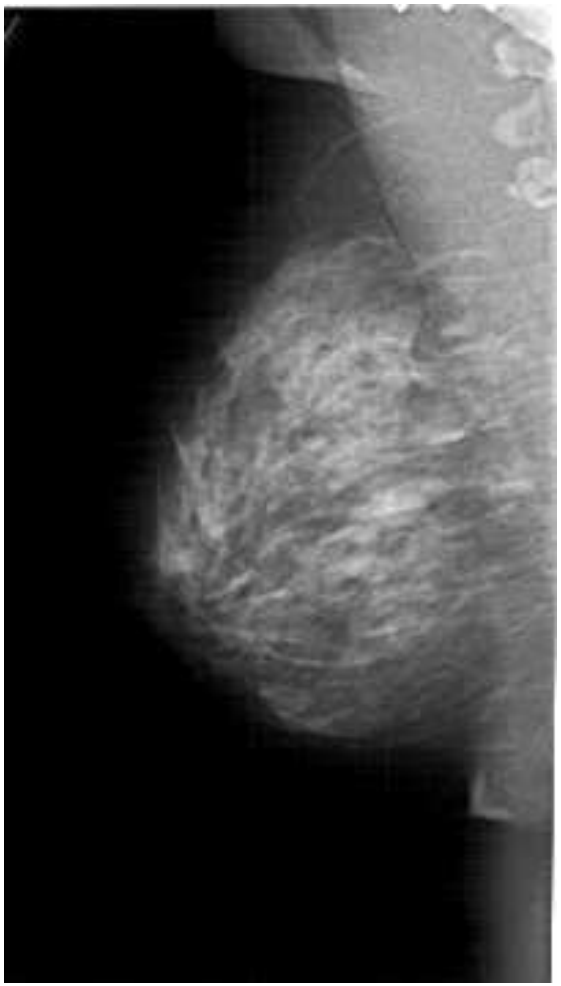

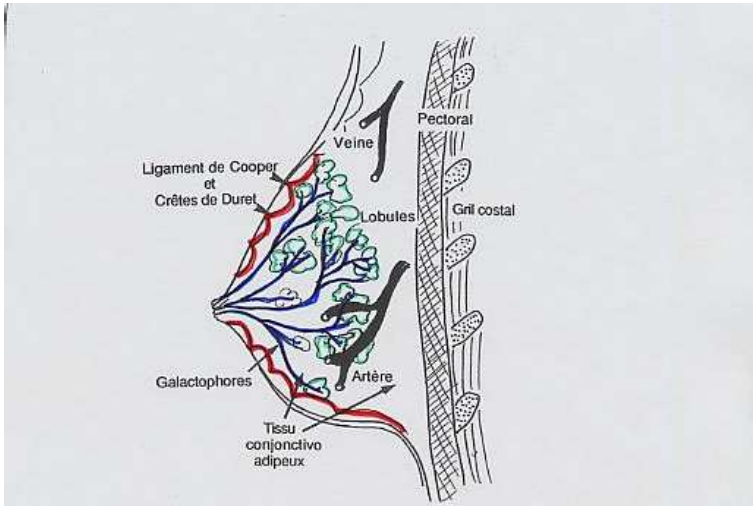

FIG. 1-1 *a.* – *Anatomie simplifiée.*

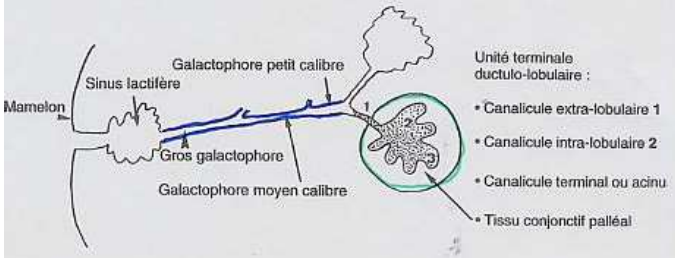

FIG. 1-1 *b.* – *Unité terminale ductulo-lobulaire, selon Wellings.*

What is breast cancer ?

- malignant tumor of mammal gland
- incidence : 30000 new case each year in France
- prevention is very difficult (as opposed to lung cancer)
- hereditarity : 5 to 10 % only (BRCA1/2 genes)
- forecast depends on the tumoral volume at diagnosis

$\Rightarrow$ **SCREENING** using mammography

Radiological anomalies

- Opacities

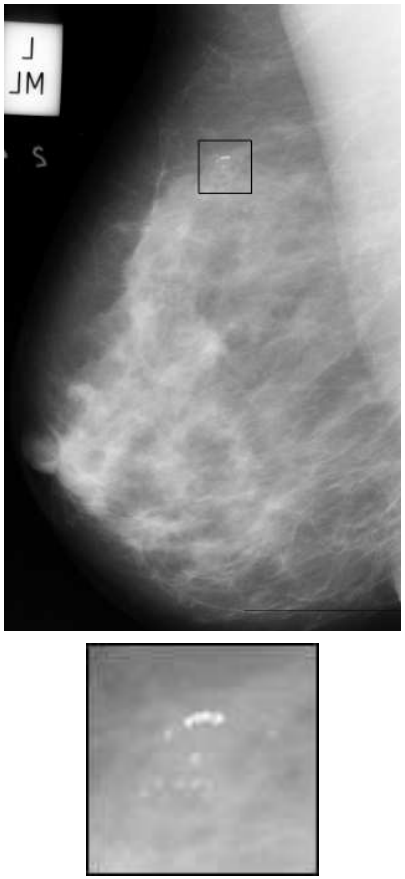

- Calcifications

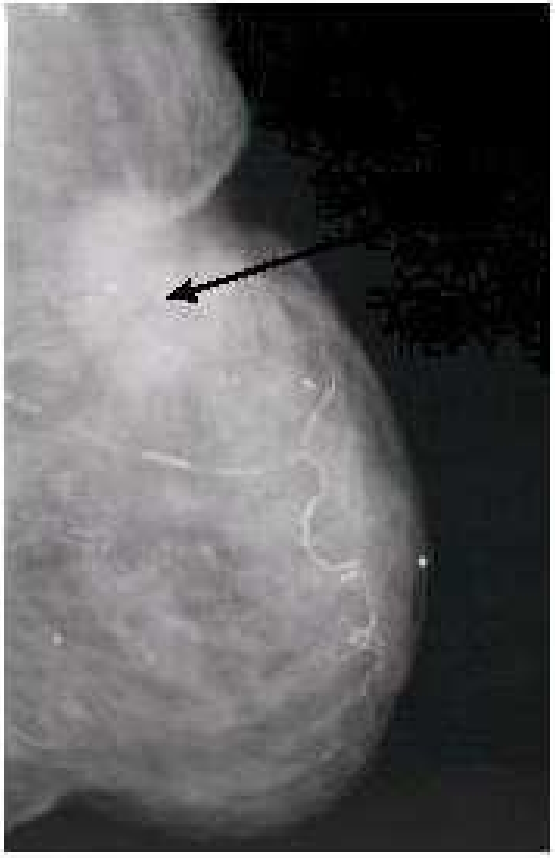

- Architectural distorcions

Digitalized mammographies : texture analysis

- **dense breasts : more difficult to diagnose**
- **only 2 classes of monofractal properties**

Digital Database for Screening Mammography:

`http://marathon.csee.usf.edu/Mammography/Database.html`

Dense breast

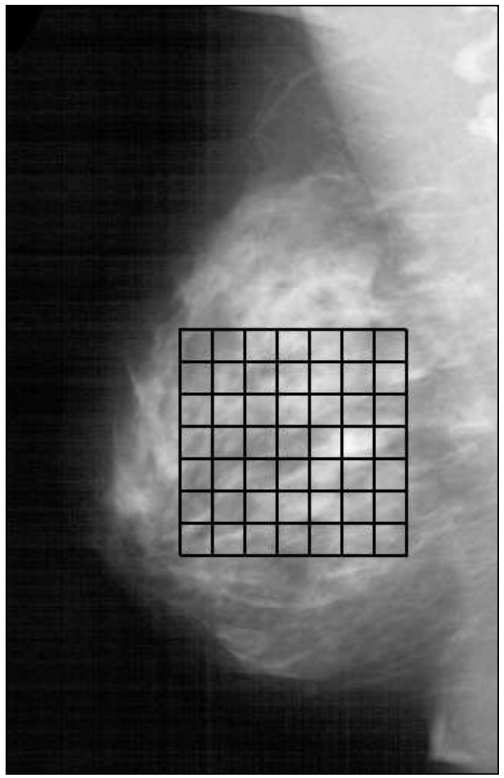

Fatty breast

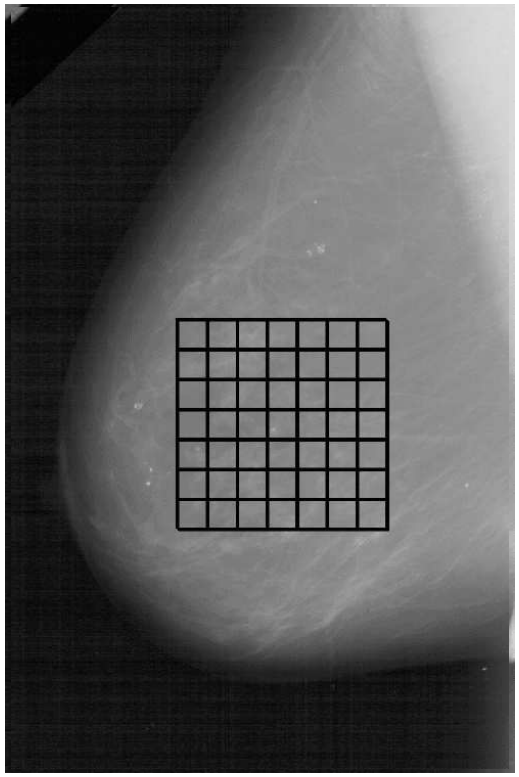

Application of 2D WTMM methodology in mammography

Tissue classification : dense

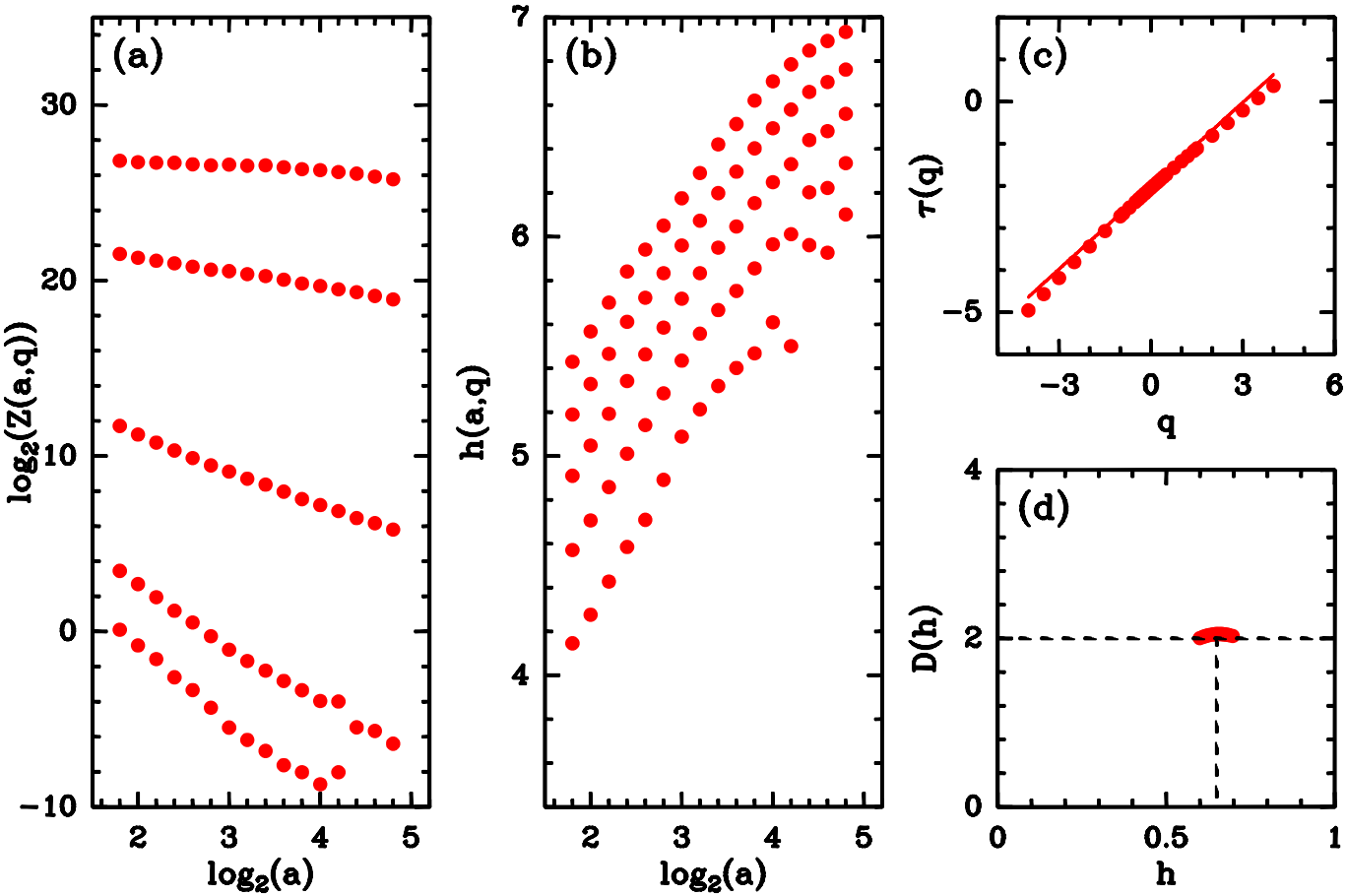

- **Dense** breast : monofractal, $H = 0.65$ **persitent** correlations

Application of 2D WTMM methodology in mammography

Tissue classification : dense vs fatty

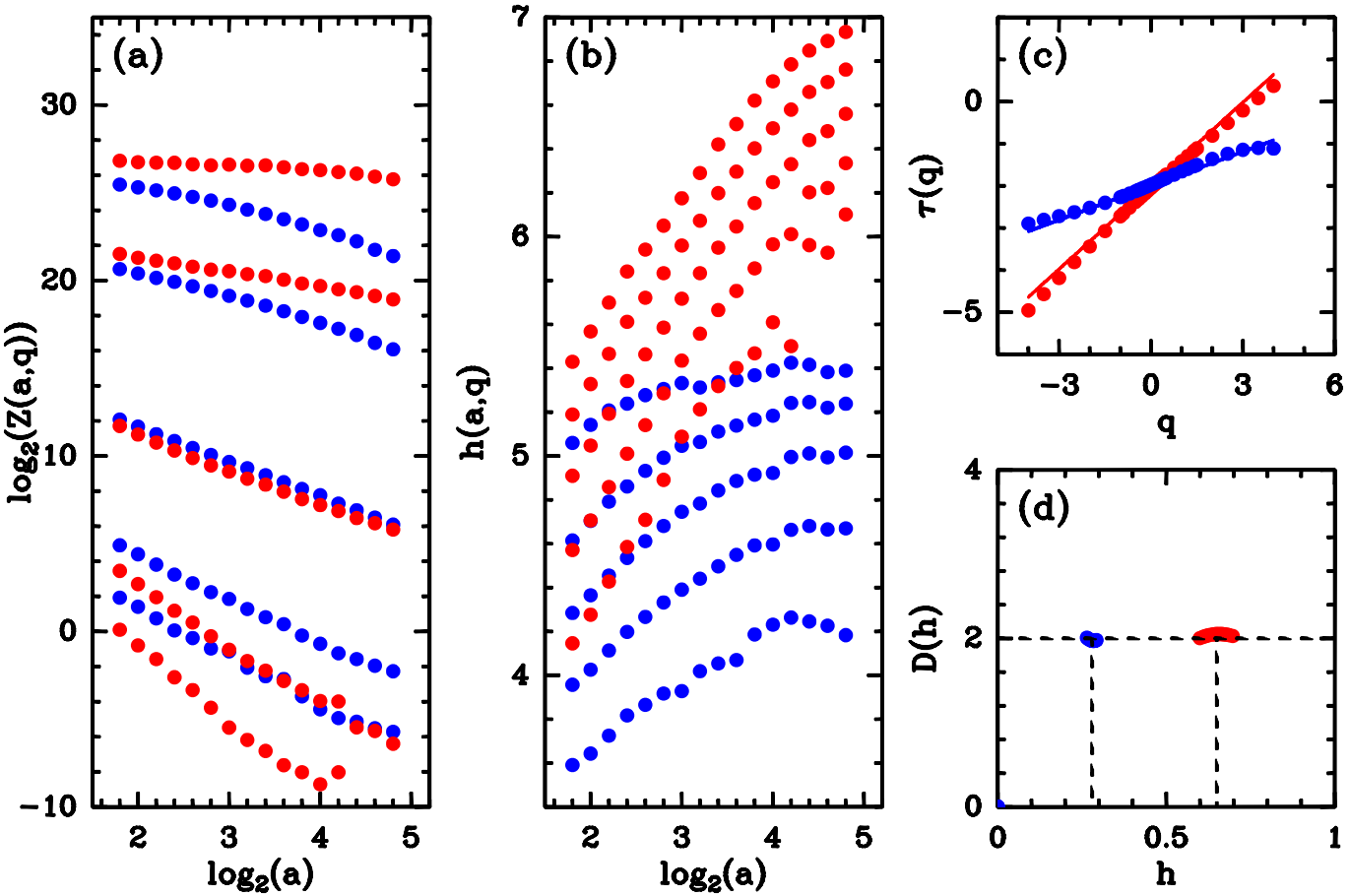

- Dense breast : monofractal, $H = 0.65$ persitent correlations
- Fatty breast : monofractal, $H = 0.30$ anti-persitent correlations

Application to digitalized mammographies

Colored Maps :
segmentation of dense $h > 0.52$ areas and fatty $h < 0.38$ areas

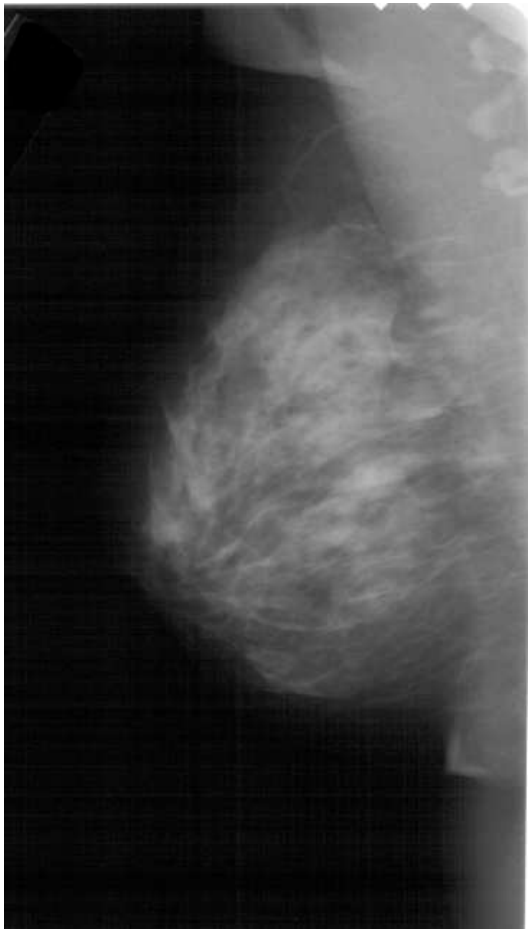

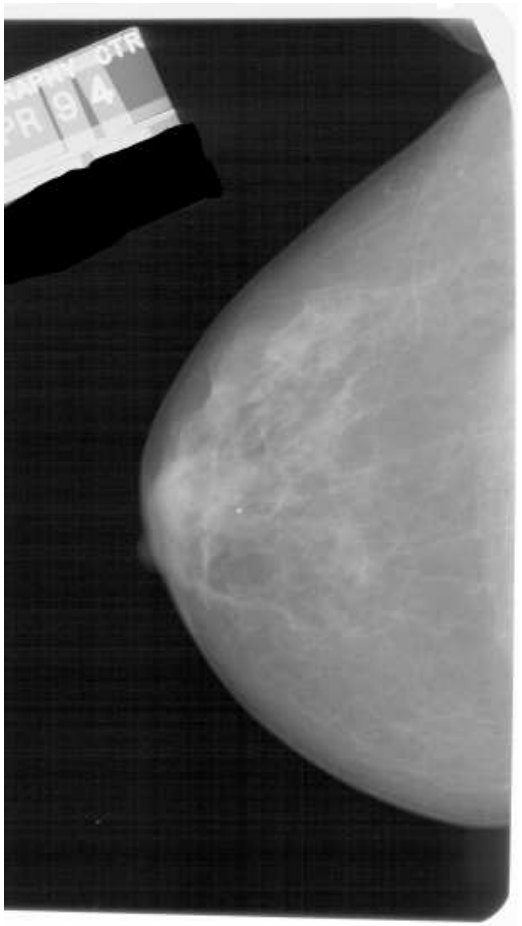

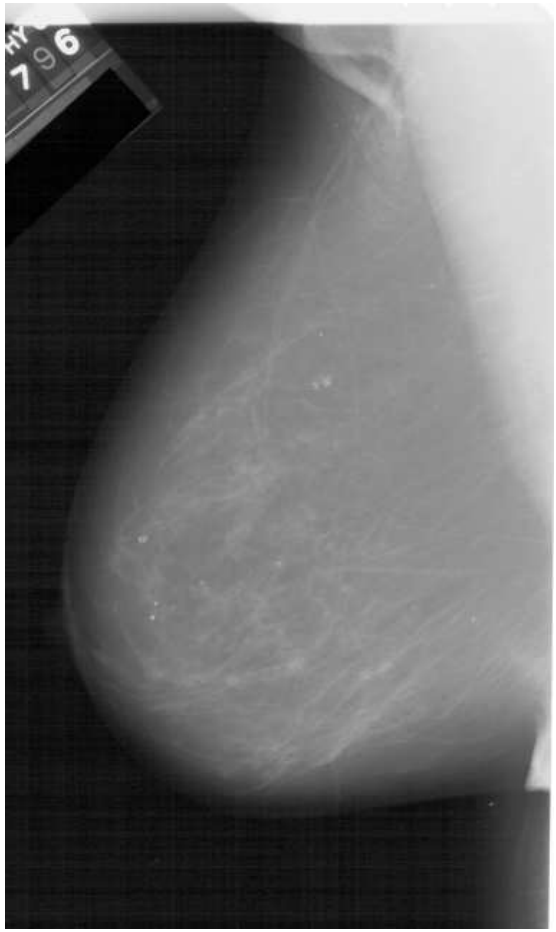

Application to digitalized mammographies

Colored Maps :
segmentation of dense $h > 0.52$ areas and fatty $h < 0.38$ areas

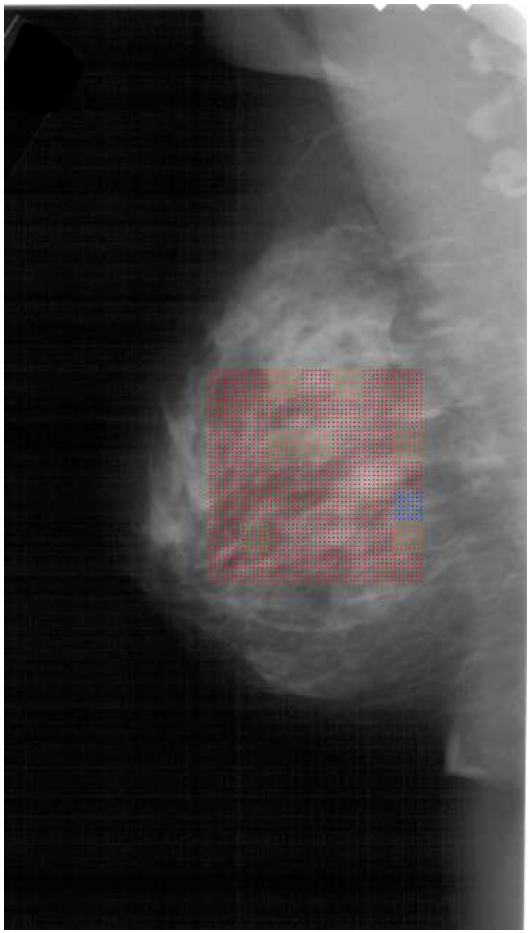

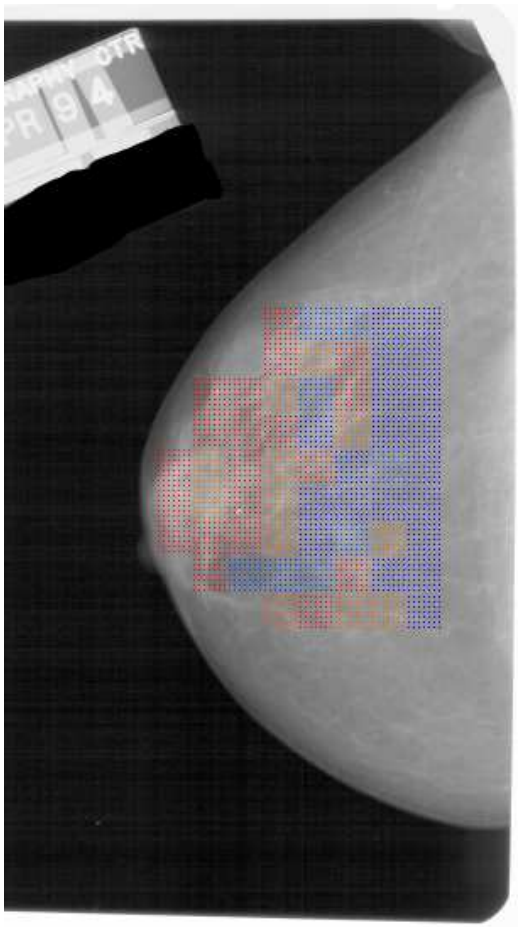

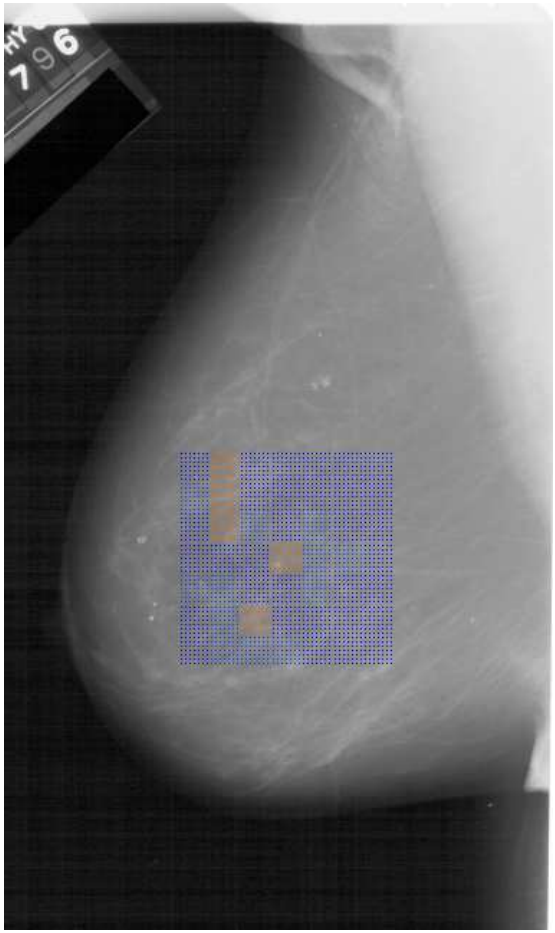

Microcalcifications detection

Segmentation of WT skeleton lines :
microcalcifications vs background texture

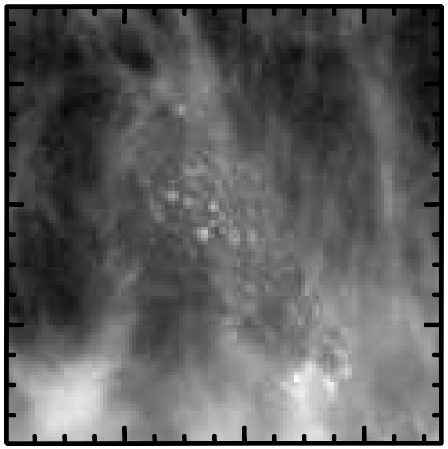

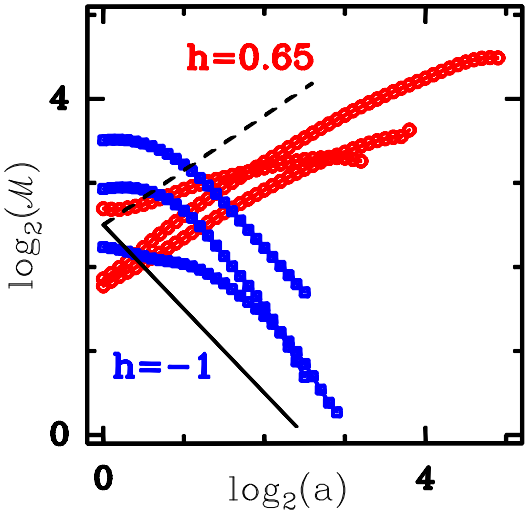

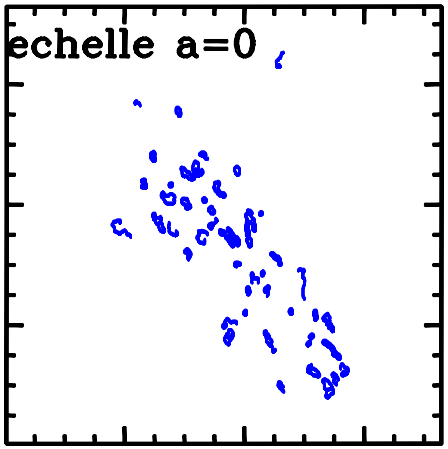

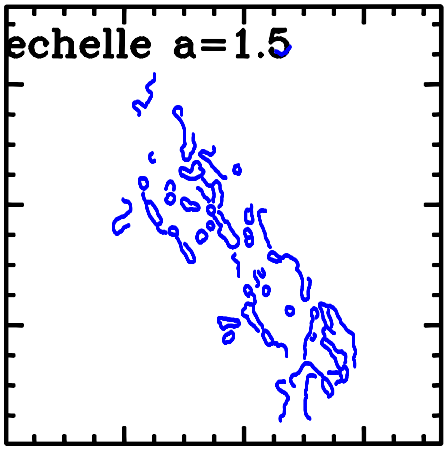

- Background lines
- Microcalcifications

  almost-punctual objects behave like 'Dirac' shapes ($h = -1$)

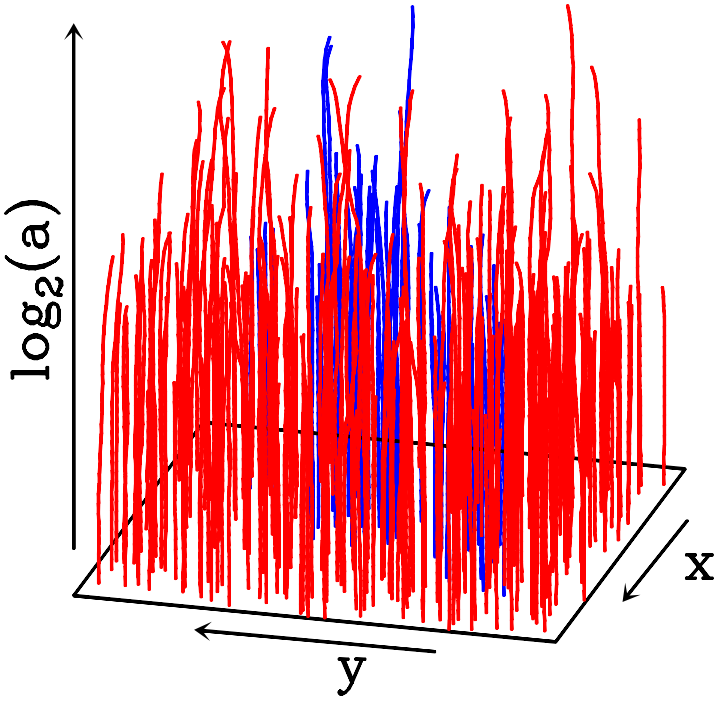

Cluster of microcalcifications

Study of microcalcification spatial distribution

Partition functions :

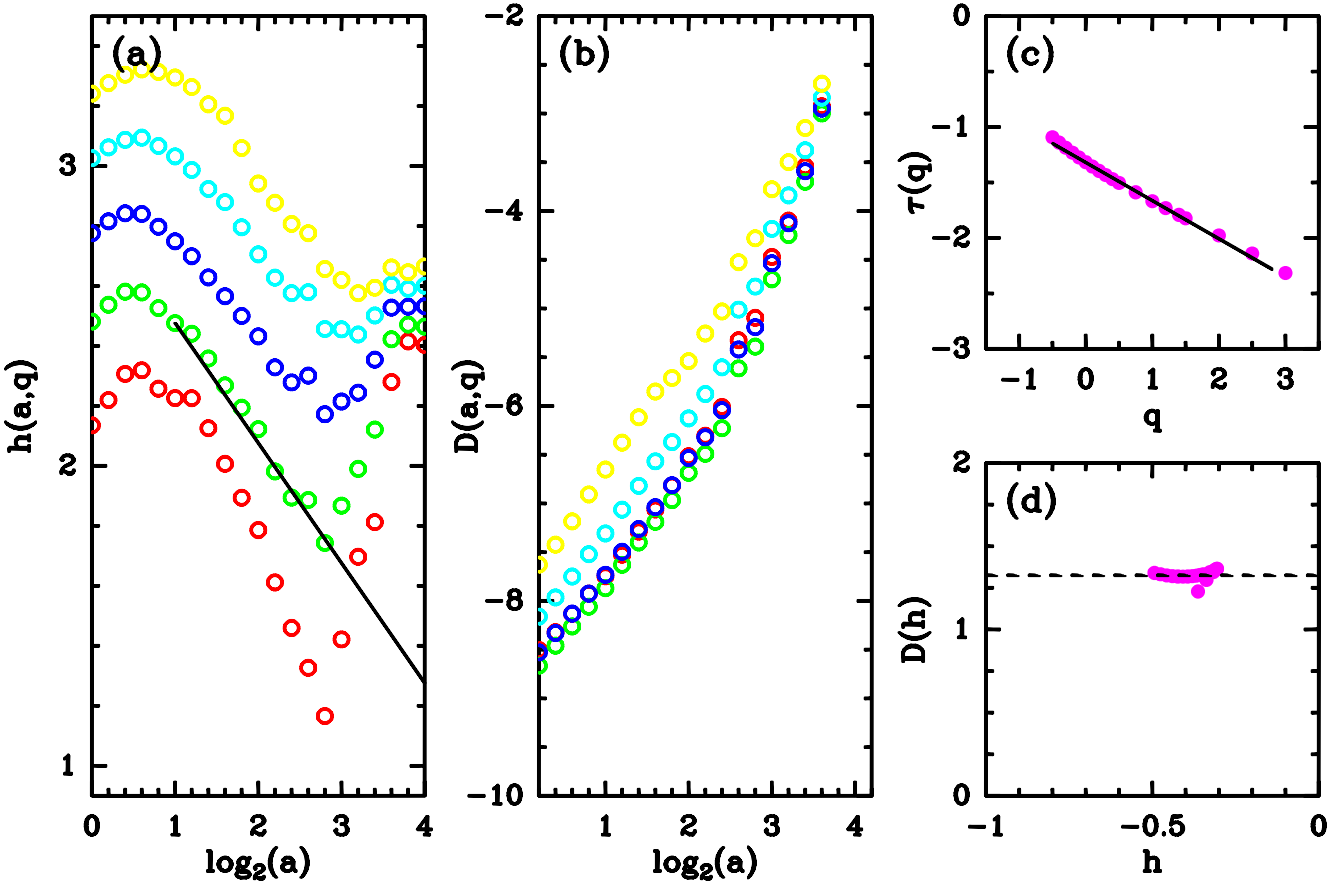

$$D_F = 1.3$$

observation :

fractal ramifi cation of cluster of microcalcifi cations $(1 < D_F < 2)$ seems to be correlated to the pathology's malignancy

Conclusions and prospects (1)

- the 2D WTMM method provides a framework for an automated measure of the breast radio-density and for studying the fractal geometry of clusters of microcalcifications.
- further study is necessary to validate quantitatively how far measuring the fractal dimension D_F could improve computer-aided diagnosis systems benign/malignant